CMD Workshop 35 : Spintronics course
in Center for Spintronics Research Network (CSRN),
Graduate School of Engineering Science, Osaka University.

September 3, 2019

Spintronic Interface design

(スピントロニクス・インターフェース・デザイン)

Yoshio Miura

National Institute for Materials Science (NIMS)

Research Center for Magnetic and Spintronic Materials (CMSM)

Spin Theory Group

Topics

0. Introduction on spintronics

1. First-Principles Study on magneto-crystalline anisotropy of Fe/MgO(001) and Fe/$MgAl_2O_4$(001)

K. Masuda and Y. Miura, PRB **98**, 224421 (2018).

2. First-Principles Study on magnetic damping of Fe/MgO(001)

Y. Miura, in preparation

3. First-Principles Study on Anisotropic Magneto-Peltier Effect

K. Masuda, K.-i. Uchida, R. Iguchi, Y. Miura PRB **99**, 104406 (2019)

Instroduction

Magnetic tunnel junction (MTJs)

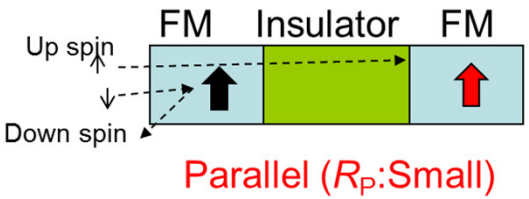

Parallel (R_P:Small)

(FM: Ferromagnetic metal)

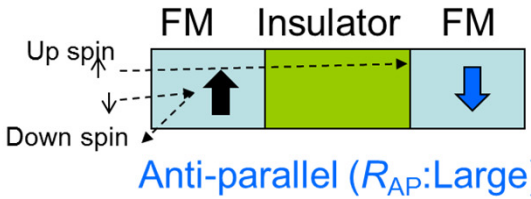

Anti-parallel (R_{AP}:Large)

Tunneling magnetoresistance (TMR)

$$\text{TMR ratio} = \frac{R_{AP} - R_P}{R_{AP}}$$

Magnetoresistive Random Access Memory (MRAM)

- Non volatile memory
- Fast writing speed (10～50ns)
- Low electricity consumption (～30μW)
- Long endurance (10 years)

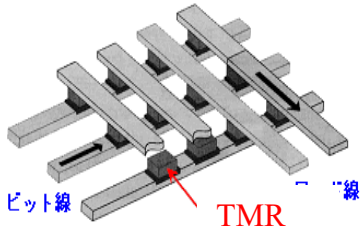

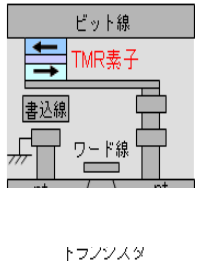

Everspin
64Mbit MRAM

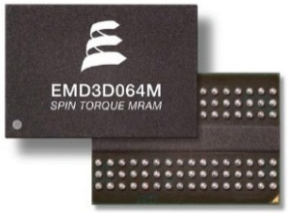

Magnetic censer

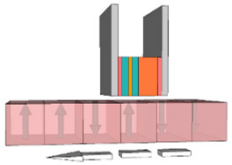

HDD read-out-head

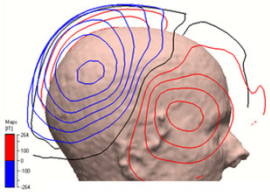

Earth's magnetic field censer・current censer for car・biomagnetic censer

Corresponding to SQUID

Magnetization reversal in MTJs

1. Magnetic field by current

problem : ・complicate circuit.
・current∝1/device-size

Effects of demagnetizing field increase the critical current for writing with decreasing size of device

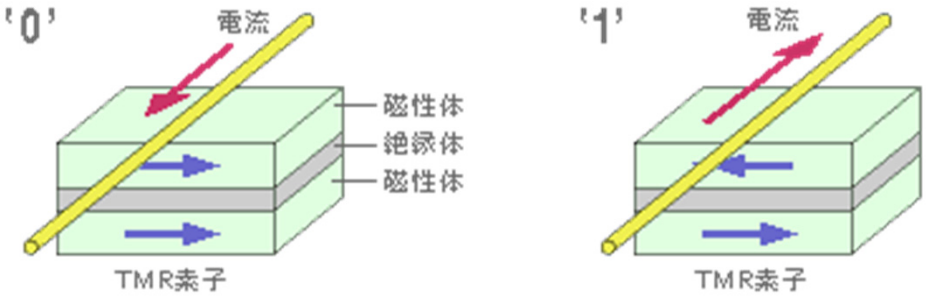

2. Spin transfer torque（STT）

The spin flip of conductive electron give the torque to the local spin moment due to the angular momentum conservation

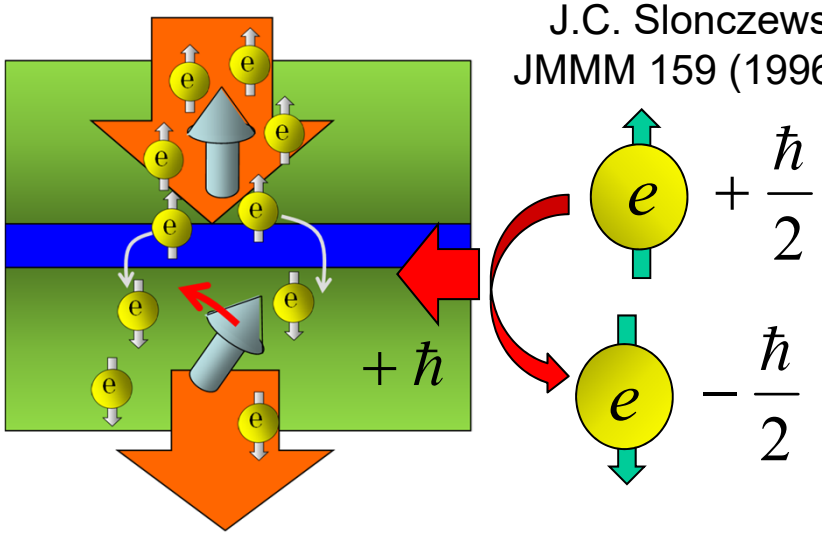

J.C. Slonczewski, JMMM 159 (1996) L1.

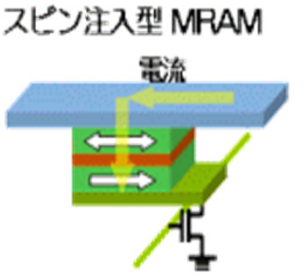

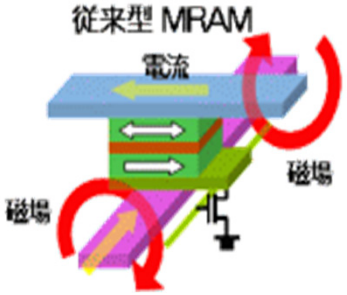

・simple circuit
・current∝device-size

Tohoku Univ. Ando lab. HP

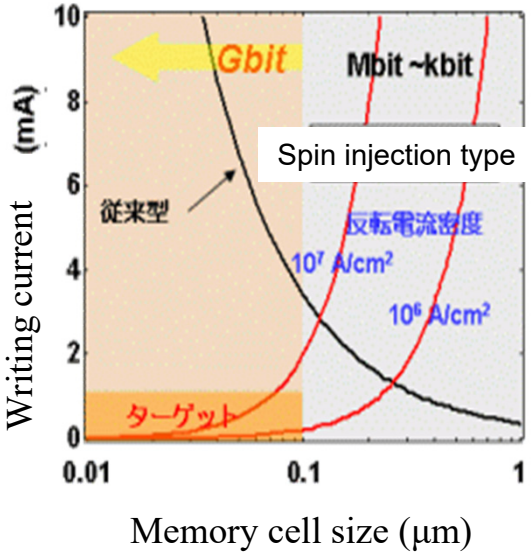

Magnetization reversal in MTJs

3. Domain wall motion type

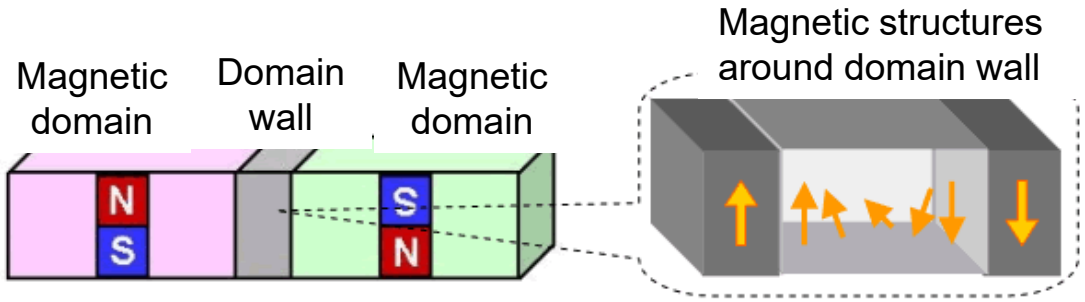

http://www.jst.go.jp/pr/announce/20060301/index.html

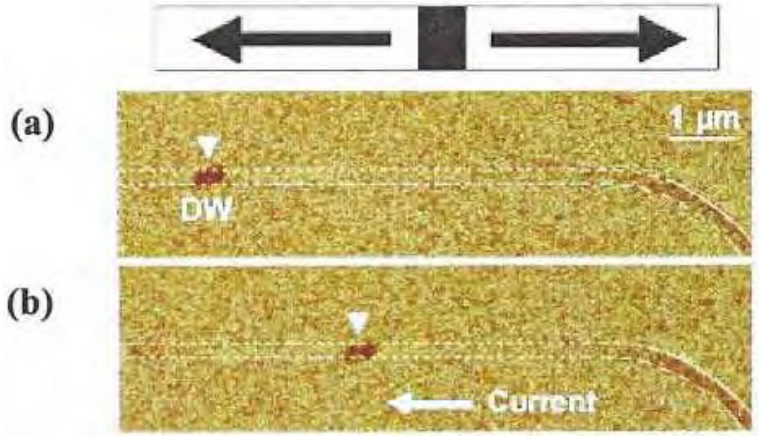

M. Hayashi,et.al. PRL92,077205 (2007)

- Fast and stable magnetization reversal was realized in experiments

Parallel magnetization

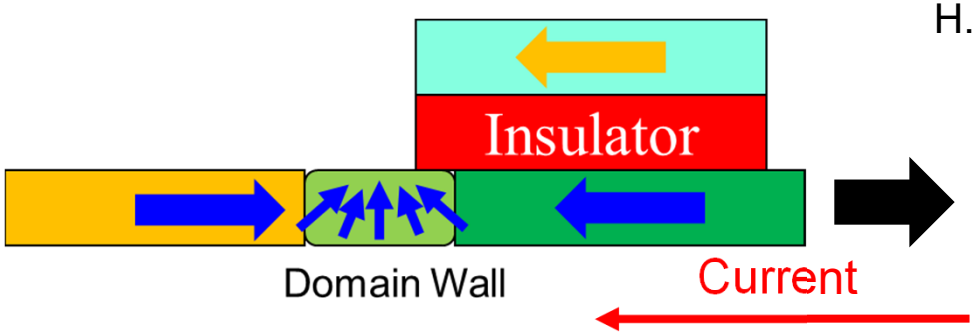

Anti-Parallel magnetization

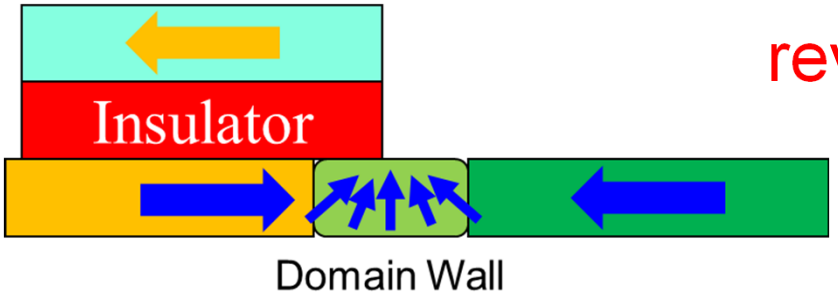

H. Tanigawa, et al., Appl. Phys. Exp. **4**, 013007 (2011).

（3-terminal device）

⇒Faster magnetization reversal with low energy consumption

Voltage-driven dynamic switching in MTJ

Applied Physics Express **9**, 013001 (2016)
http://doi.org/**10.7567/APEX.9.013001**

Evaluation of write error rate for voltage-driven dynamic magnetization switching in magnetic tunnel junctions with perpendicular magnetization

Yoichi Shiota*, Takayuki Nozaki, Shingo Tamaru, Kay Yakushiji, Hitoshi Kubota, Akio Fukushima, Shinji Yuasa, and Yoshishige Suzuki

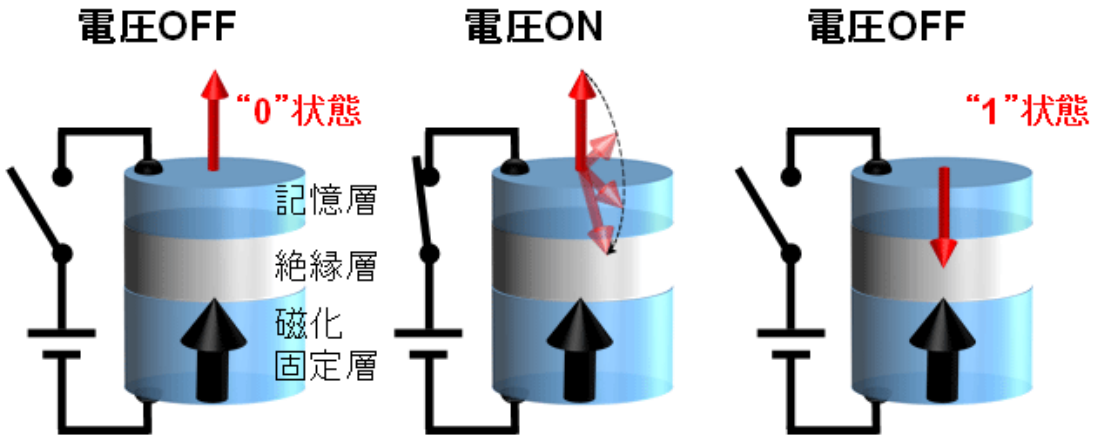

From website of Sahashi's ImPACT project in JST

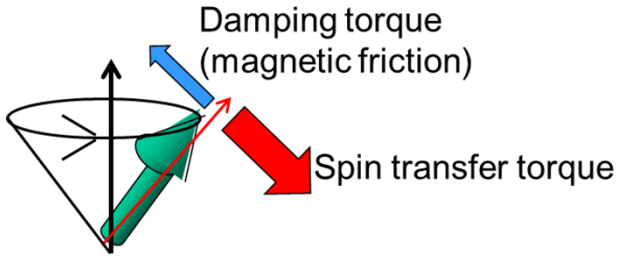

Write Error Rate (WER)

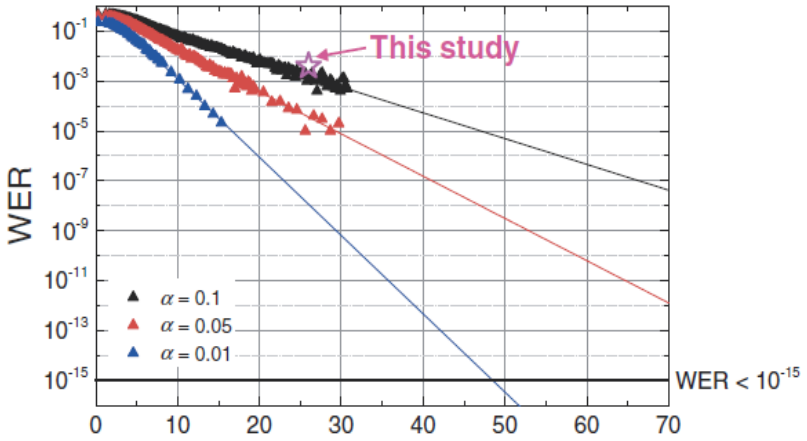

Fig. 4. Calculated WER as a function of Δ for fixed tilted magnetization angle and half precession period τ_{pulse} for various damping constants.

Pulsed bias voltage changes PMA of interface of FM layer and promote the precession motion of the magnetization.

➡ By removing the voltage with a proper pulse duration, such as a half precession period, magnetization switching can be achieved.

➡ Basically, no current flow

Large Ku and Small damping α can reduce the WER

Magnetization reversal by spin transfer torque (STT)

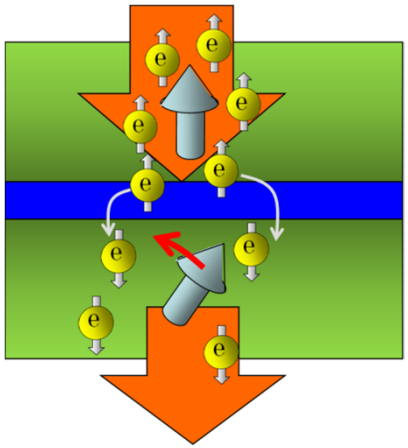

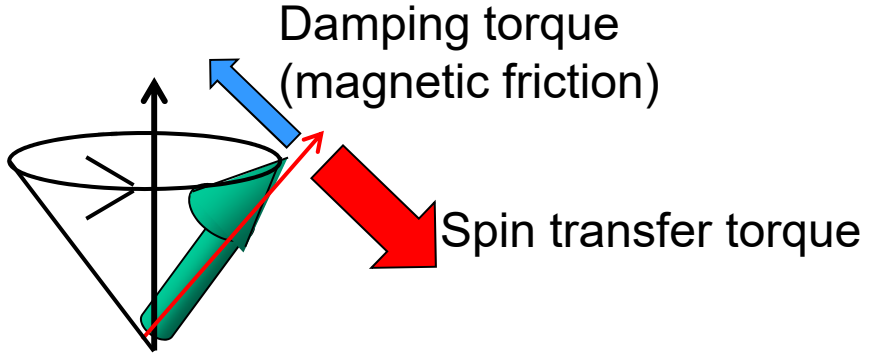

Reduction of critical current density (J_{c0})

$(10^7 \mathrm{A/cm^2} \Rightarrow 10^5 \mathrm{A/cm^2})$

$$J_{c0} \propto \alpha M_S [H_{\mathrm{anti}} \pm 4\pi M_S]\ t/P$$

J.C. Slonczewski, JMMM 159 (1996) L1.

α: Magnetic damping constant
M_S: Saturation Magnetization
$H_{\mathrm{anti}} \pm 4\pi M_S$: Effective anisotropy field
P: Spin polarization
t: Thickness of FM layer

1. High spin polarization (P)

2. Low damping constant(α)

3. Perpendicular magnetic anisotropy(PMA) H_{anti}-$4\pi M_s$

Topics

0. Introduction on spintronics

1. First-Principles Study on magneto-crystalline anisotropy of Fe/MgO(001) and Fe/$MgAl_2O_4$(001)

K. Masuda and Y. Miura, PRB **98**, 224421 (2018).

2. First-Principles Study on magnetic damping of Fe/MgO(001)

Y. Miura, in preparation

3. First-Principles Study on Anisotropic Magneto-Peltier Effect

K. Masuda, K.-i. Uchida, R. Iguchi, Y. Miura PRB **99**, 104406 (2019)

Thermal stability of magnetization in MTJs

To achieve ultra high density MRAM

In-plane MTJ

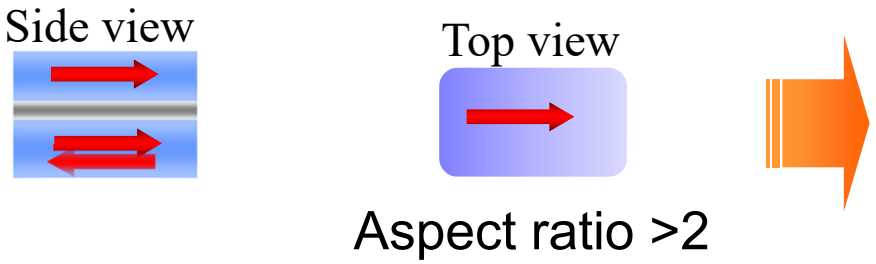

Perpendicular MTJ

For 10 year's write endurance

Thermal stability factor $\frac{K_u V}{k_B T} \geq 60$

K_u : uniaxial magnetic anisotropy

Large K_u is required with decreasing volume towards scaling down of device dimensions

Examples of Perpendicular MTJ

Using $L1_0$-type FePt, CoPt, CoFePd alloys and its multilayered structures

[1] M. Yoshikawa, *et al.*, IEEE Trans. Magn. vol.**44** 2573 (2008). (Toshiba)

[2] K. Yakushiji, *et al.*, APEX vol. **3** 053003 (2010). (AIST)

[3] K. Mizunuma *et al.*, APEX vol. **4** 023002 (2011). (Tohoku)

Interfacial Perpendicular Magnetic Anisotropy (PMA) for MgO

S. Ikeda, *et al*., Nature Materials **9**, 721 (2010).

- CoFeB/MgO/CoFeB(001)

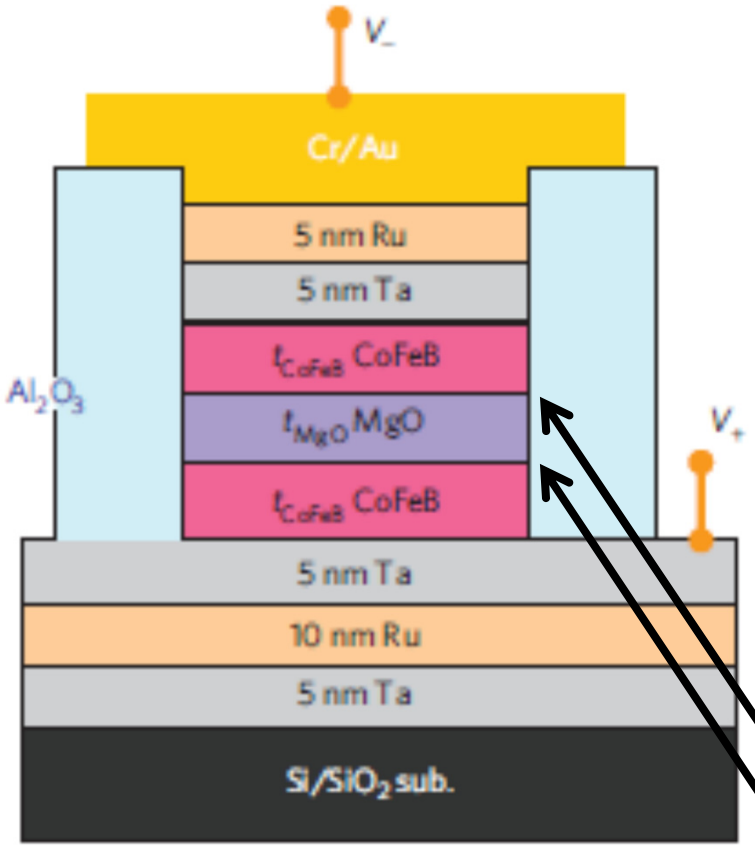

TMR ratio of 120% at 300K

In-plane magnetization (t_{CoFeB}=2.0nm)

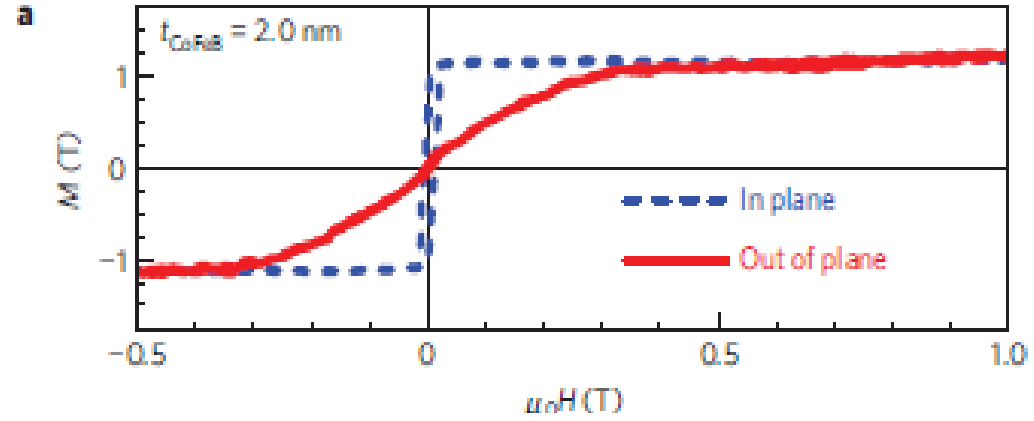

Perpendicular magnetization (t_{CoFeB}<1.3nm)

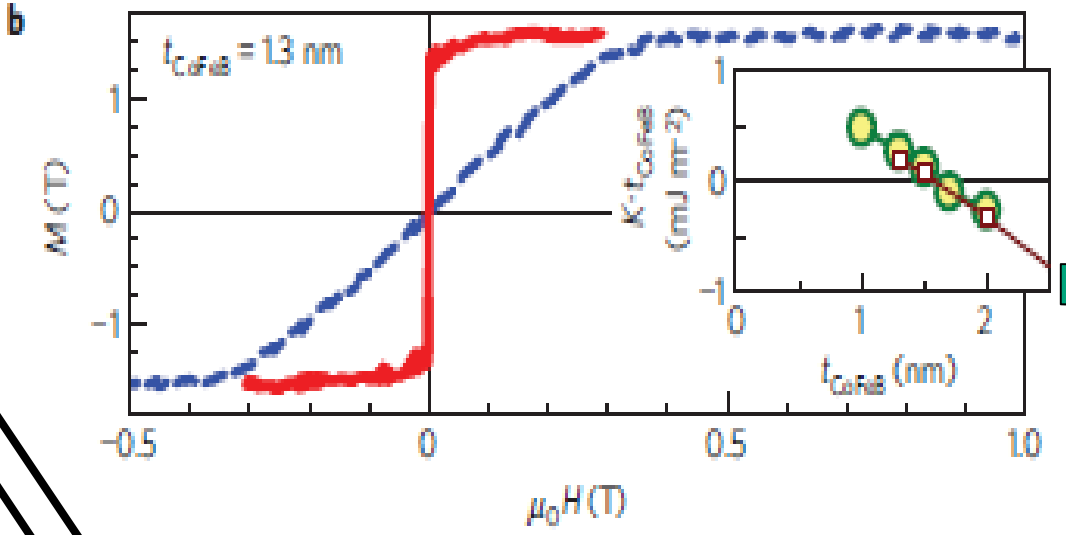

Interfacial perpendicular MCA of Fe/MgO(001), which is K_i=1.30 mJ/m^2

Interfacial PMA for $MgAl_2O_4$

Multilayer structure

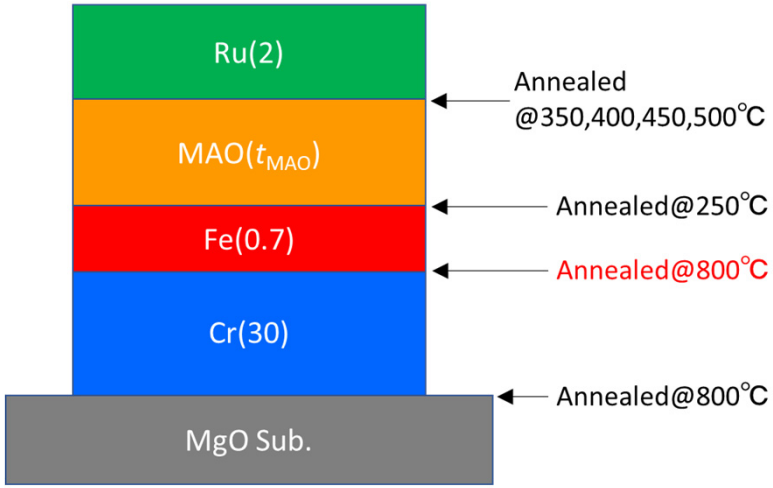

Post-annealing temperature for a Cr buffer
: key to obtain large PMA

RHEED patterns

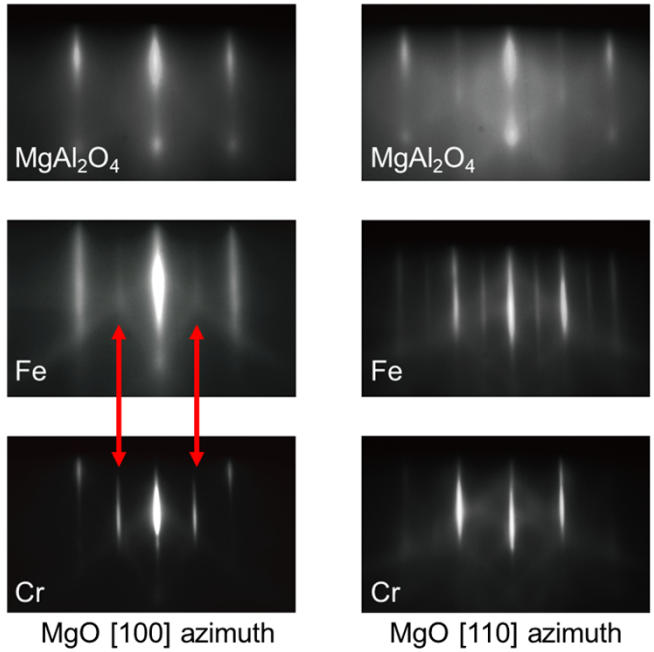

Annealing temp. dependence of K_{eff}

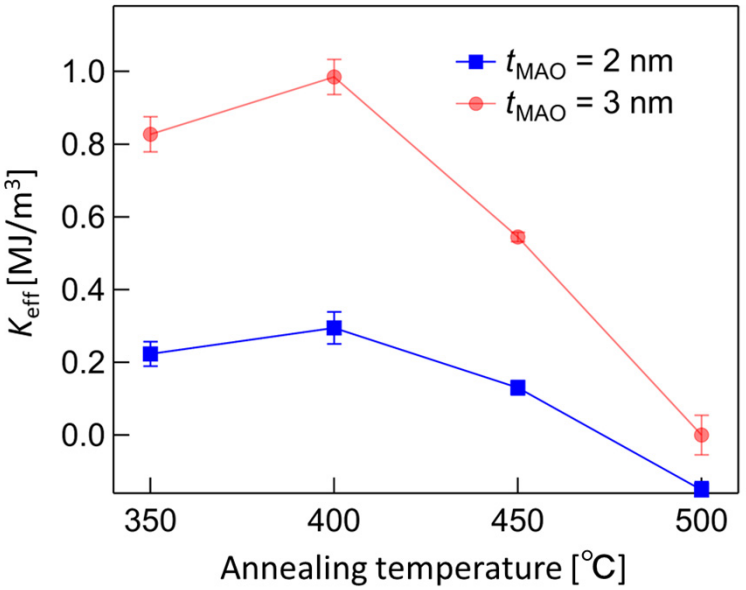

M-H loops (largest PMA case)

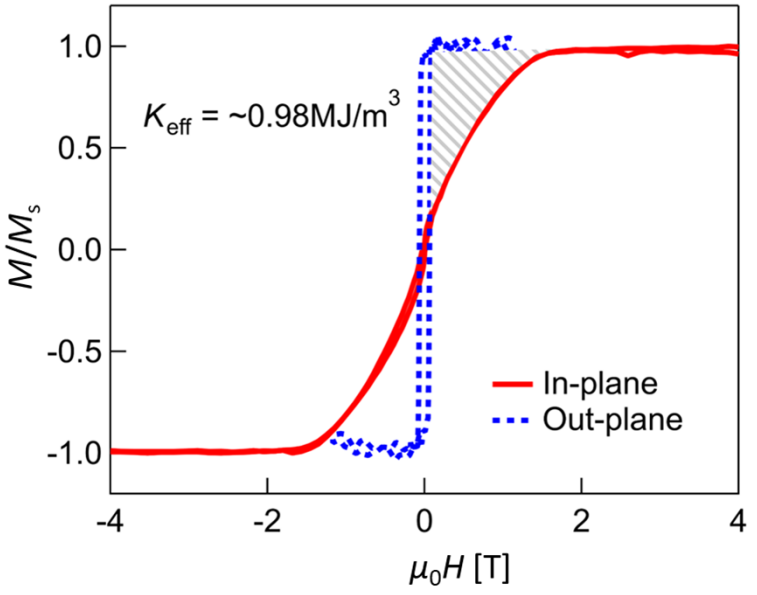

Q. Xiang, *et al.*, APEX **11**, 063008 (2018).

Calculation results

Calculation: VASP-PAW-PBE, 37x37x1 (19x19x1) k-points for Fe/MgO (Fe/$MgAl_2O_4$)

K. Masuda and Y. Miura, PRB **98**, 224421 (2018).

	K_i (mJ/m^2)	$E_{demag}t$ (mJ/m^2)	$K_{eff}t=K_i-E_{demag}t$ (mJ/m^2)	$\Delta M_{orb,i}$ (μ_B/atom)	K_i (mJ/m^2) Experiments
Fe/$MgAl_2O_4$($a=a_{Fe}$)	1.192	-0.895	0.296	0.026	-
Fe/MgO($a=a_{MgO}/\sqrt{2}$)	1.617	-0.828	0.788	0.030	1.30 [1]
Fe/MgO($a=a_{Fe}$)	1.552	-0.908	0.643	0.020	0.98 [2]

- Bruno's relation holds for all cases
- PMA of Fe/$MgAl_2O_4$ is slightly smaller than that of Fe/MgO, which is consistent with experimental results.

[1] S. Ikeda, *et al.*, Nature Materials **9**, 721 (2010).

[2] Q. Xiang, *et al.*, APEX **11**, 063008 (2018).

Second order perturbation of spin-orbit interaction (SOI)

P. Bruno, PRB **39**, 865 (1989). G. Laan, JPCM **10**, 3239 (1998).

$$E_\eta^{(2)} = -\sum_{\text{exc}} \frac{\left|\langle \text{exc}\,|H_{\text{SO}}|\,\text{gr}\rangle\right|^2}{\varepsilon_{\text{exc}} - \varepsilon_{\text{gr}}}$$

$$H_{\text{SO}} = \xi \vec{L}\cdot\vec{S}$$

$$|\text{gr}\,(\text{exc})\rangle = \sum_{\mu,\sigma} c_{i,\mu,\sigma}|i,\mu\rangle$$

η:direction of spin (x or z)

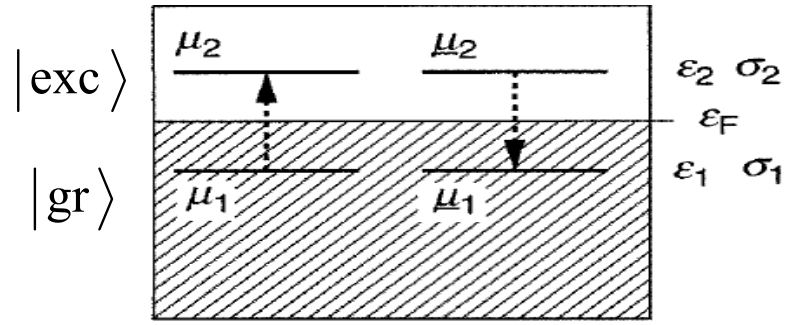

μ: local atomic orbital index

i,j: index of atomic position

$$E_\eta^{(2)}(i) = \xi_i \sum_{\mu_1,\mu_2,\underline{\mu_1},\underline{\mu_2}} \left\langle \underline{\mu_1}\uparrow \left|\vec{L}\cdot\vec{S}\right| \underline{\mu_2}\uparrow \right\rangle_\eta \left\langle \mu_2\uparrow \left|\vec{L}\cdot\vec{S}\right| \mu_1\uparrow \right\rangle_\eta$$

$$\times \sum_j \xi_j \left[G_{\mu_1,\underline{\mu_1}}^{\mu_2,\underline{\mu_2}}(\uparrow,\uparrow;i,j) + G_{\mu_1,\underline{\mu_1}}^{\mu_2,\underline{\mu_2}}(\downarrow,\downarrow;i,j) - G_{\mu_1,\underline{\mu_1}}^{\mu_2,\underline{\mu_2}}(\uparrow,\downarrow;i,j) - G_{\mu_1,\underline{\mu_1}}^{\mu_2,\underline{\mu_2}}(\downarrow,\uparrow;i,j) \right]$$

Joint Local DOS

$$G_{\mu_1,\underline{\mu_1}}^{\mu_2,\underline{\mu_2}}(\sigma_1,\sigma_2;i,j) = \int_{\varepsilon_1<E_F<\varepsilon_2} \frac{d\varepsilon_1 d\varepsilon_2}{\varepsilon_2-\varepsilon_1} \sum_{\text{k}} n_{\mu_1,\underline{\mu_1},\sigma_1}^{i,j}(\text{k},\varepsilon_1) n_{\mu_2,\underline{\mu_2},\sigma_2}^{i,j}(\text{k},\varepsilon_2)$$

Magneto-crystalline anisotropy energy(MAE)

$$\Delta E_{\text{MCA}}^{(2)}(i) = E_{\text{z}}^{(2)}(i) - E_{\text{x}}^{(2)}(i)$$

$$\sum_{n'}^{unocc} c_{i\mu'\sigma'}^{kn'*} c_{j\lambda'\sigma'}^{kn'} \delta(\epsilon' - \epsilon_{kn'\sigma'}^{(0)})$$

We directly estimated the second-order perturbative contribution of MCA energy depending on each atomic site and spin-transition process.

ξ_{Fe}=50meV

Second order perturbation for MAE analysis

Magneto-crystalline anisotropy energy(MAE)

$$\Delta E^{(2)} = \sum_{o,u} \frac{\left|\langle o|\lambda \vec{L}\cdot\vec{S}|u\rangle\right|^2}{\varepsilon_u - \varepsilon_o} = \Delta E^{(2)}_{\text{up}\leftarrow\text{up}} + \Delta E^{(2)}_{\text{up}\leftarrow\text{down}} + \Delta E^{(2)}_{\text{down}\leftarrow\text{up}} + \Delta E^{(2)}_{\text{down}\leftarrow\text{down}}$$

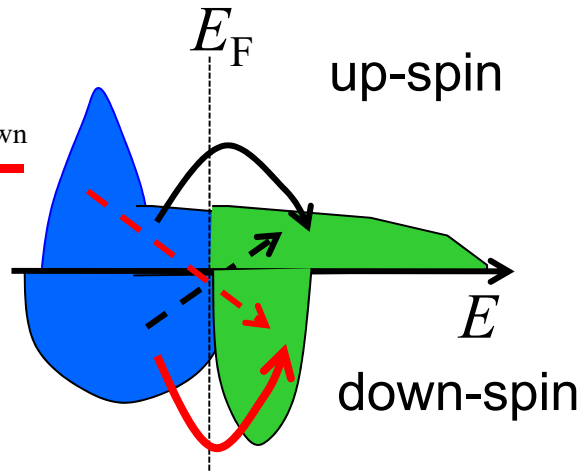

$$\left.\begin{aligned}\Delta E^{(2)}_{\text{up}\leftarrow\text{up}} &\approx 0\\ \Delta E^{(2)}_{\text{up}\leftarrow\text{down}} &\approx 0\end{aligned}\right\}$$

For more than half 3d-TM, up-spin *d* states are fully occupied.

$$\Delta E^{(2)}_{\text{down}\leftarrow\text{up}} = \lambda^2 \sum_{o^+,u^-} \frac{\left|\langle o^+|L_x|u^-\rangle\right|^2}{\varepsilon_{u^-} - \varepsilon_{o^+}} - \lambda^2 \sum_{o^+,u^-} \frac{\left|\langle o^+|L_z|u^-\rangle\right|^2}{\varepsilon_{u^-} - \varepsilon_{o^+}}$$

≈0, in case of large exchange coupling

$$\Delta E^{(2)}_{\text{down}\leftarrow\text{down}} = \lambda^2 \sum_{o^-,u^-} \frac{\left|\langle o^-|L_z|u^-\rangle\right|^2}{\varepsilon_{u^-} - \varepsilon_{o^-}} - \lambda^2 \sum_{o^-,u^-} \frac{\left|\langle o^-|L_x|u^-\rangle\right|^2}{\varepsilon_{u^-} - \varepsilon_{o^-}}$$

$$L_z Y_l^m = m Y_l^m$$

Contributed to perpendicular MAE, if there are *d* orbitals with same magnetic quantum number (*m*) around E_F

$$L_x Y_l^m \propto Y_l^{m\pm 1}$$

Contributed to in-plane MAE, if there are *d* orbitals with *m* and m±1 exist around E_F.

Matrix elements		
Cartesian	Band notation	$\langle L_\sigma \rangle$ value
$\langle xz\|L_z\|yz\rangle$	$\langle 5''\|L_z\|5'\rangle$	1
$\langle x^2-y^2\|L_z\|xy\rangle$	$\langle 3\|L_z\|4\rangle$	2
$\langle z^2\|L_x\|yz\rangle$	$\langle 1\|L_x\|5'\rangle$	$\sqrt{3}$
$\langle xy\|L_x\|xz\rangle$	$\langle 4\|L_x\|5''\rangle$	1
$\langle x^2-y^2\|L_x\|yz\rangle$	$\langle 3\|L_x\|5'\rangle$	1
$\langle z^2\|L_y\|xz\rangle$	$\langle 1\|L_y\|5''\rangle$	$\sqrt{3}$
$\langle xy\|L_y\|yz\rangle$	$\langle 4\|L_y\|5'\rangle$	1
$\langle x^2-y^2\|L_y\|xz\rangle$	$\langle 3\|L_y\|5''\rangle$	1

MAE vs. orbital magnetic moment (Bruno's relation)

First-order perturbative wavefunction correction by SOI

$$\delta\left|\mathrm{gr}^{(1)}\right\rangle = -\sum_{\mathrm{exc}} \frac{\left\langle \mathrm{exc}\left|\sum_I \zeta_I \vec{L}_\eta \cdot \vec{S}\right|\mathrm{gr}\right\rangle}{\varepsilon_{\mathrm{exc}} - \varepsilon_{\mathrm{gr}}}\left|\mathrm{exc}\right\rangle$$

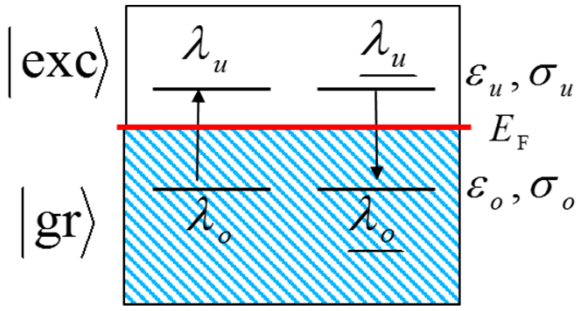

Orbital moment $\left\langle \vec{L}_\eta \right\rangle \approx \sum_{gr} \left\langle \mathrm{gr}\left|\vec{L}_\eta \cdot \delta\right|\mathrm{gr}^{(1)}\right\rangle + \mathrm{c.c.} = -\sum_{\mathrm{gr,exc}} \left\langle \mathrm{gr}\left|\vec{L}_\eta\right|\mathrm{exc}\right\rangle \frac{\left\langle \mathrm{exc}\left|\zeta\vec{L}_\eta \cdot \vec{S}\right|\mathrm{gr}\right\rangle}{\varepsilon_{\mathrm{exc}} - \varepsilon_{\mathrm{gr}}} + \mathrm{c.c.}$

$$\left\langle \vec{L}_\eta^i \right\rangle = \sum_{\lambda_o,\lambda_u,\underline{\lambda_o},\underline{\lambda_u}} \left\langle \lambda\uparrow\left|\vec{L}_\eta \cdot \vec{S}\right|\mu'\uparrow\right\rangle\left\langle \lambda'\uparrow\left|\vec{L}_\eta \cdot \vec{S}\right|\mu\uparrow\right\rangle \sum_j \zeta_j \left[G_{i,j}^{\downarrow,\downarrow}(\lambda\mu',\lambda'\mu) - G_{i,j}^{\uparrow,\uparrow}(\lambda\mu',\lambda'\mu)\right]\vec{e}_\eta$$

Orbital moment operator include only spin-conservation term, because it does not include spin operator,

2nd perturbation energy

$$E_\eta^{(2)} = \sum_i \zeta_i \sum_{\lambda\mu',\lambda'\mu} \left\langle \lambda\uparrow\left|\vec{L}\cdot\vec{S}\right|\mu'\uparrow\right\rangle\left\langle \lambda'\uparrow\left|\vec{L}\cdot\vec{S}\right|\mu\uparrow\right\rangle \times \sum_j \zeta_j \left[G_{i,j}^{\uparrow,\uparrow}(\lambda\mu',\lambda'\mu) + G_{i,j}^{\downarrow,\downarrow}(\lambda\mu',\lambda'\mu) - G_{i,j}^{\uparrow,\downarrow}(\lambda\mu',\lambda'\mu) - G_{i,j}^{\downarrow,\uparrow}(\lambda\mu',\lambda'\mu)\right]$$

$G_{i,j}^{\uparrow,\uparrow}(\lambda\mu',\lambda'\mu) \approx G_{i,j}^{\uparrow,\downarrow}(\lambda\mu',\lambda'\mu) \approx 0$

More than half

$G_{i,j}^{\uparrow,\downarrow}(\lambda\mu',\lambda'\mu)$

Large exchange coupling

Bruno's relation PRB **39**, 865 (1989).

$$\Delta E_{\mathrm{MCA}} \approx \frac{\zeta}{4}\left[m_{\mathrm{orb}}^{[001]} - m_{\mathrm{orb}}^{[100]}\right]$$

MAE of $Fe/MgAl_2O_4(001)$ by controlling lattice constant

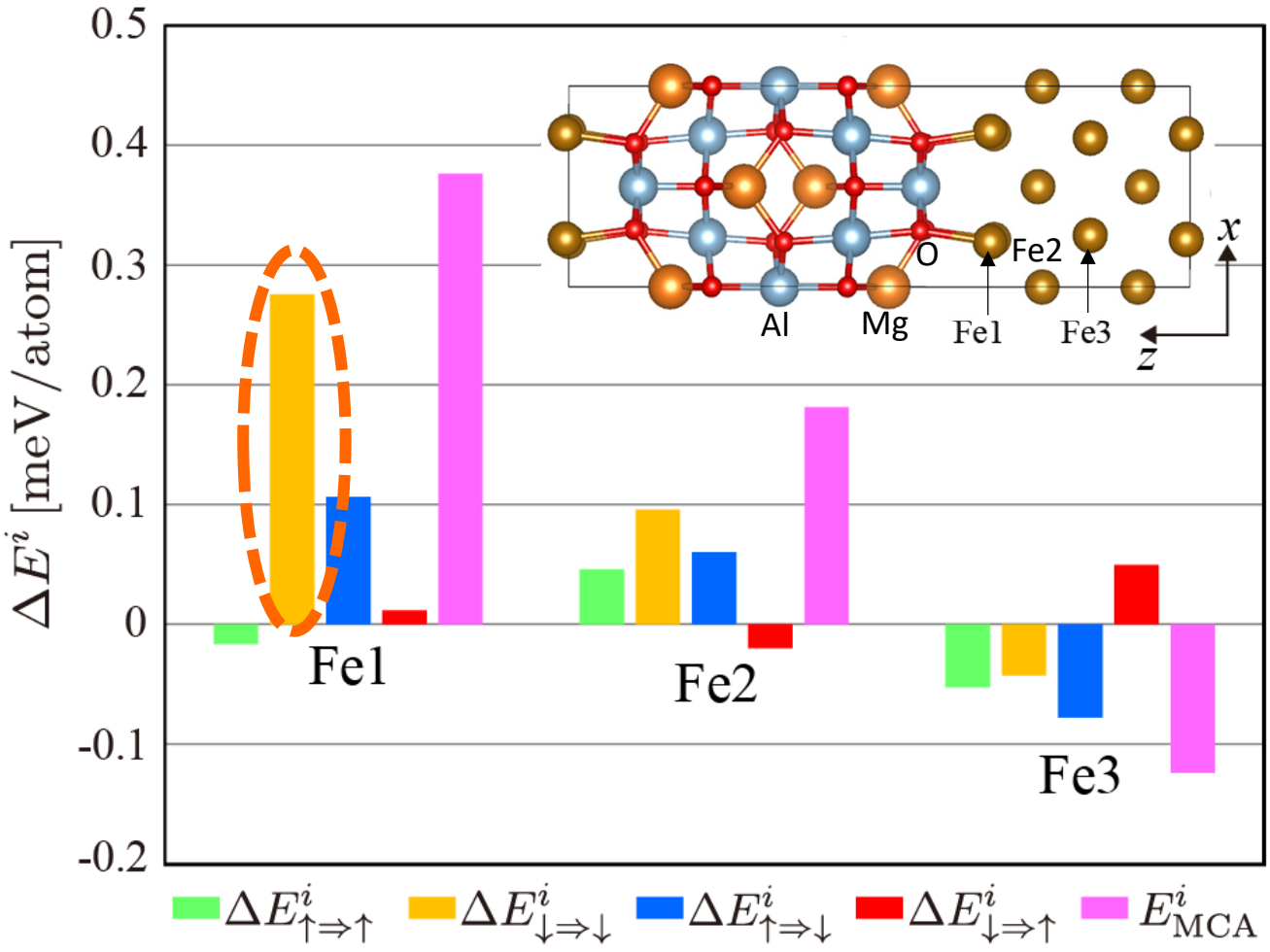

- Interfacial Fe mainly contributes to PMA
- Spin conservation term $\Delta E_{\downarrow\Rightarrow\downarrow}$ mainly contributes to PMA.

LDOS and band contribution to MAE of $Fe/MgAl_2O_4(001)$

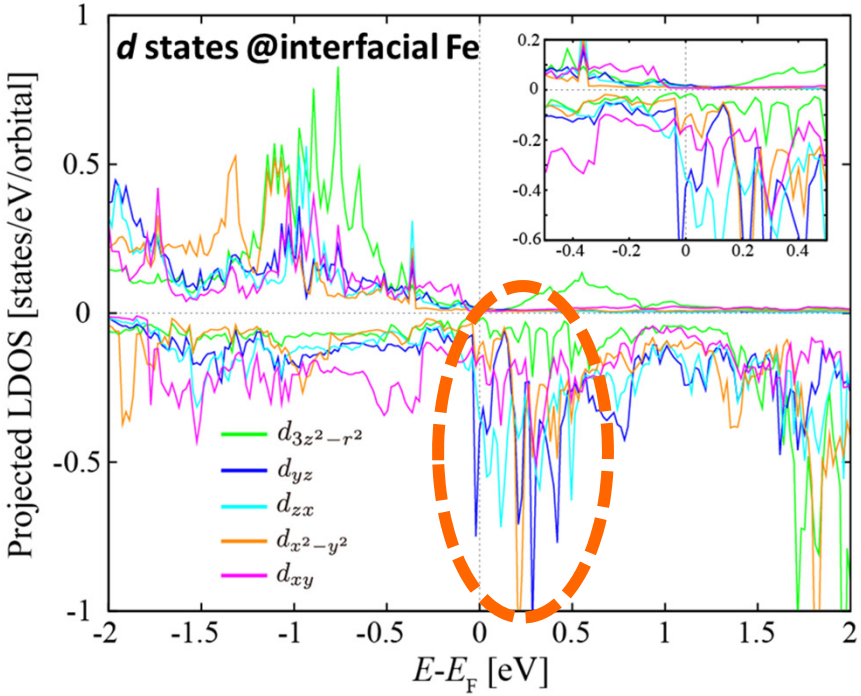

band structure of the supercell

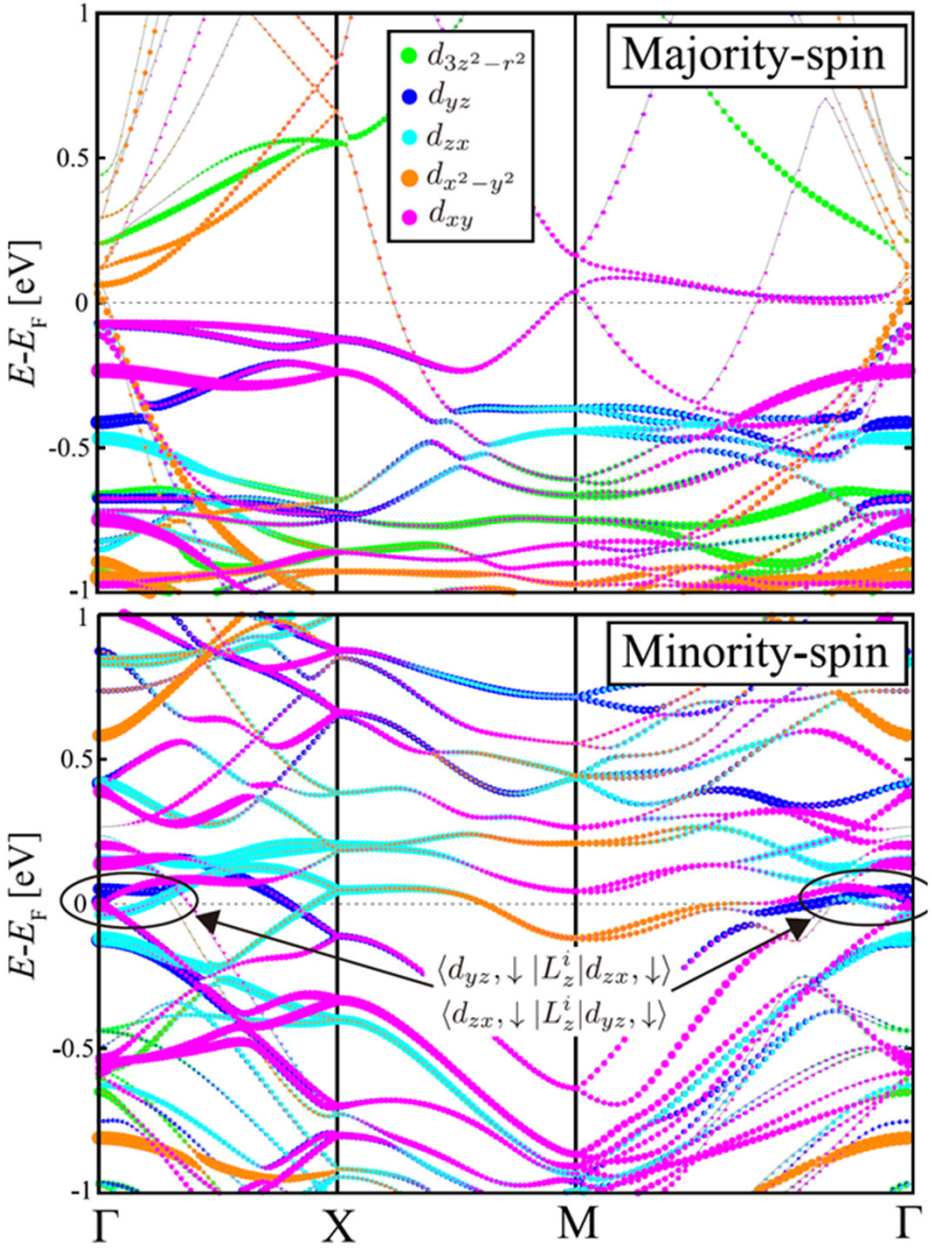

In-plane *k* dependence of MAE

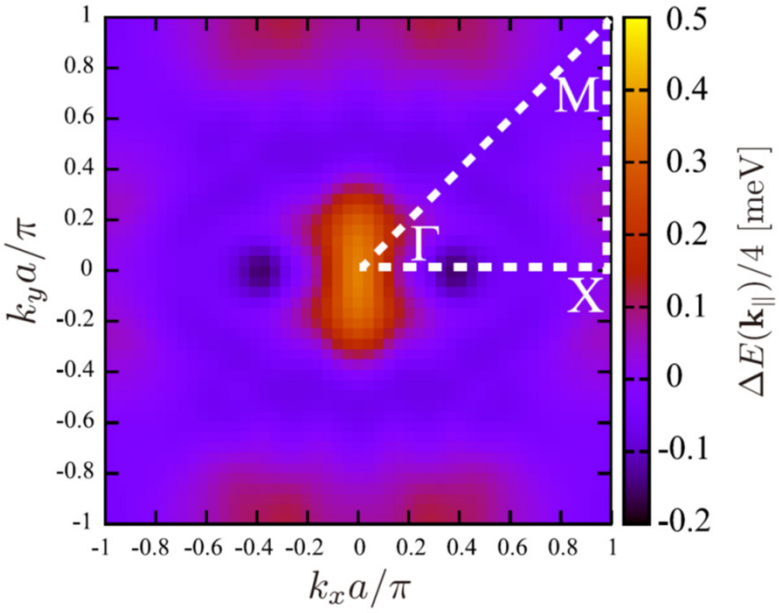

MAE of Fe/MgO(001) with changing lattice distortion

$a=a_{\mathrm{Fe}}$

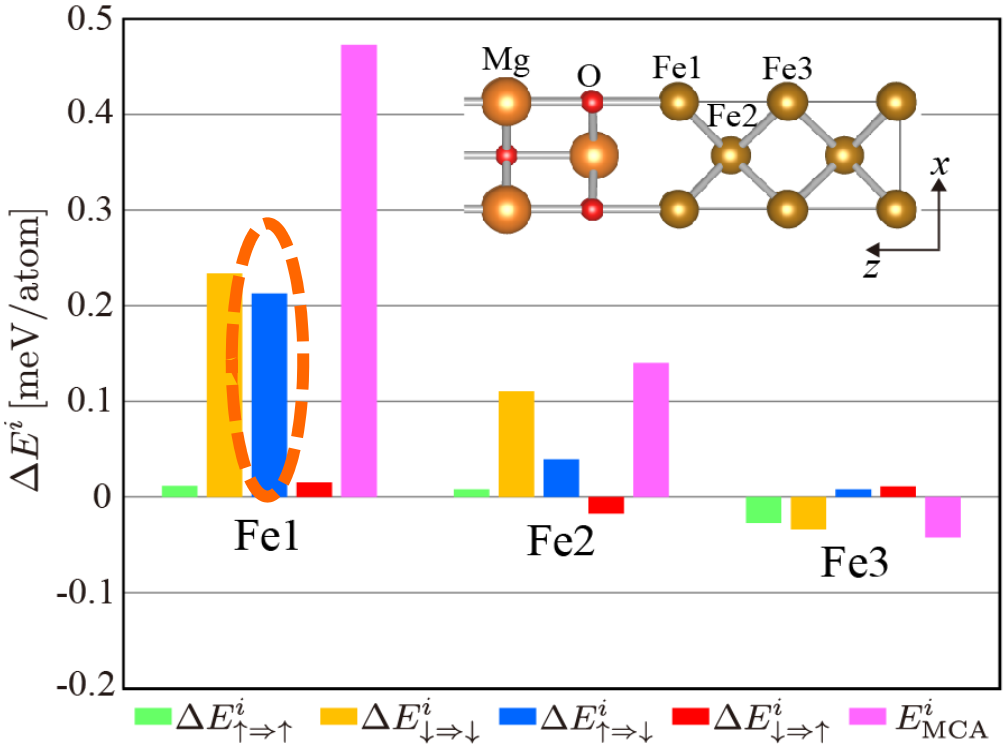

$a=a_{\mathrm{MgO}}$

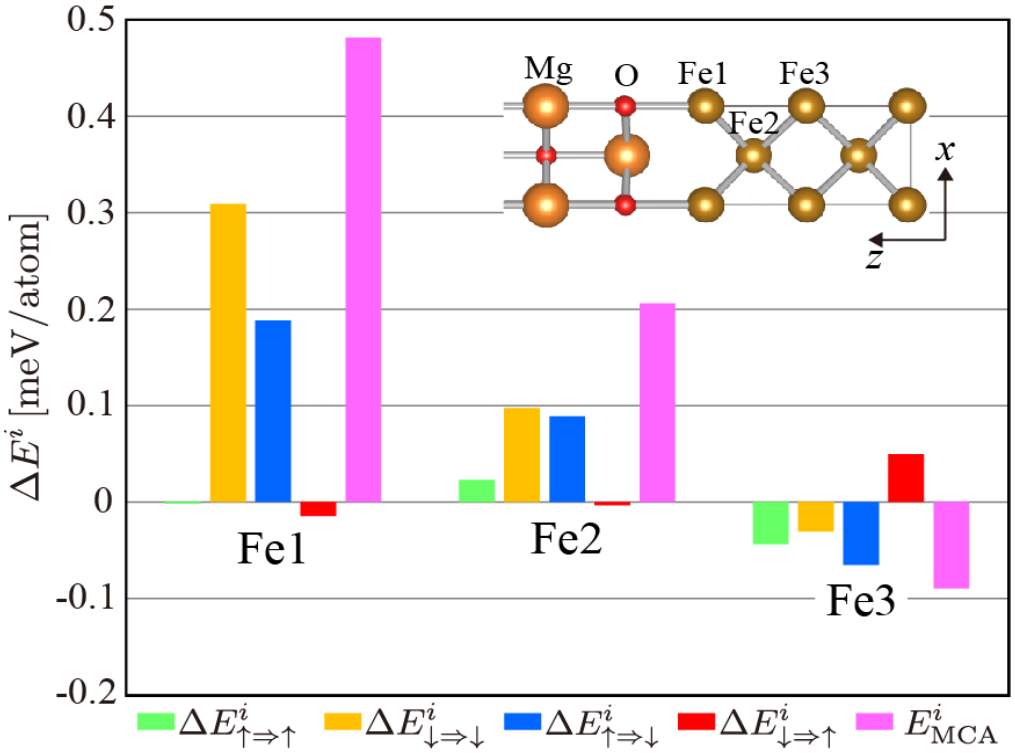

・Not only spin conservation term $\Delta E_{\downarrow\Rightarrow\downarrow}$ but also spin-flip term $\Delta E_{\uparrow\Rightarrow\downarrow}$ contributes to PMA, resulting in larger PMA than that of Fe/$MgAl_2O_4$.

・PMA of Fe/MgO(001) interfaces increases with increasing in-plane lattice constant.

Difference between $Fe/MgAl_2O_4(001)$ and Fe/MgO(001) interfaces

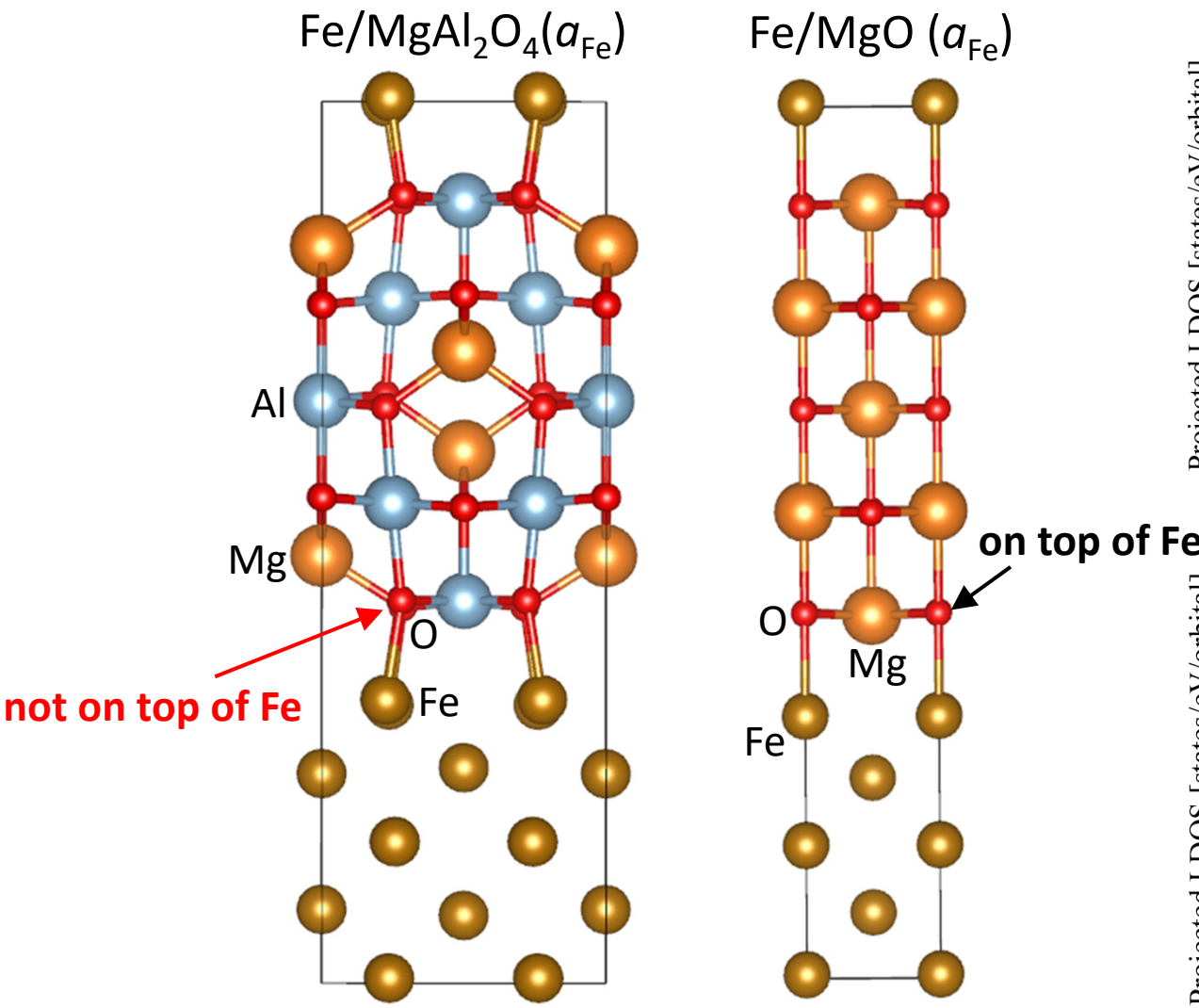

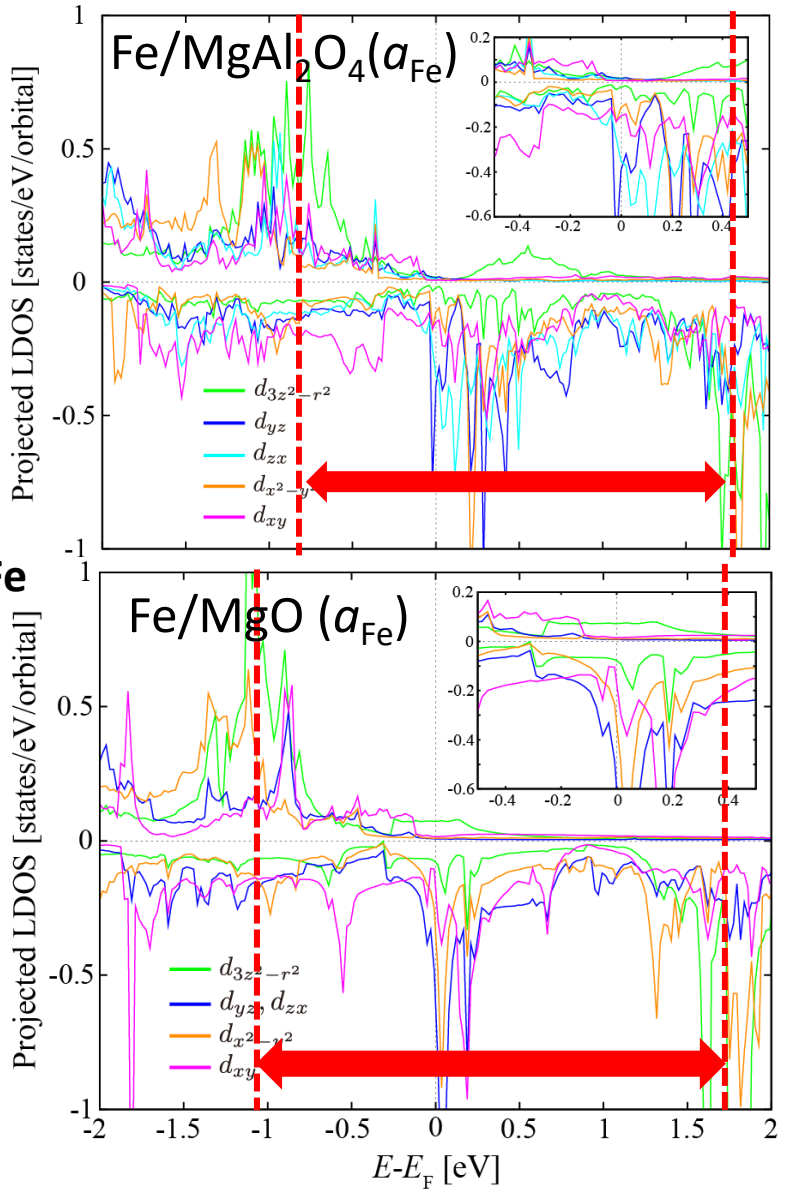

Interfacial hybridization between Fe d_{3z^2} and O p_z is different

Modification of PMA of W/Fe(001) by controlling lattice constant

Experiments

MgO sub./Cr (30nm)/W(t_W)/[Fe(2)/W(t_W)]$_4$/Cr(3 nm)

Collaboration with Prof. Okamoto in Tohoku

Appl. Phys. Express 10, 063005 (2017)

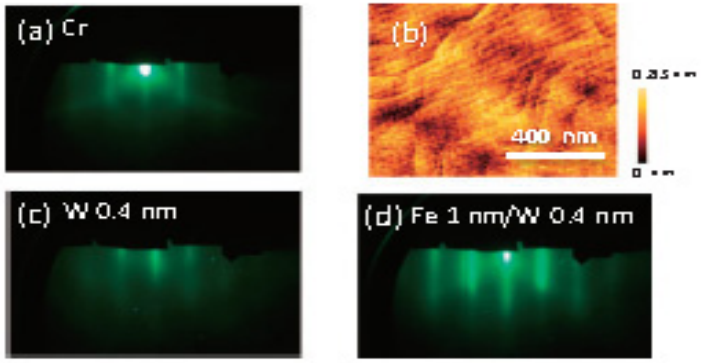

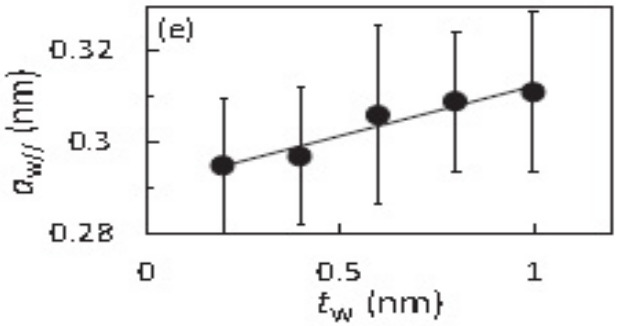

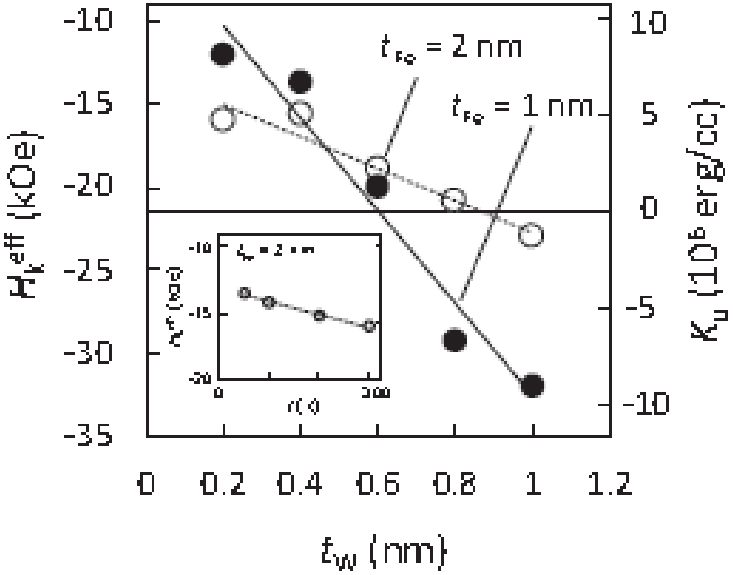

Calculation

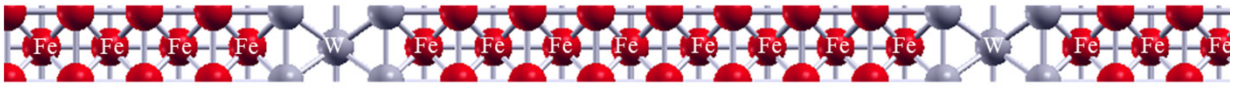

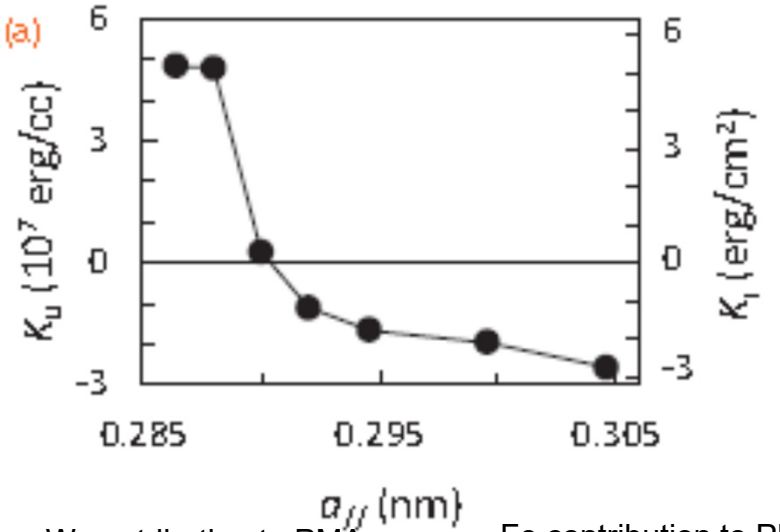

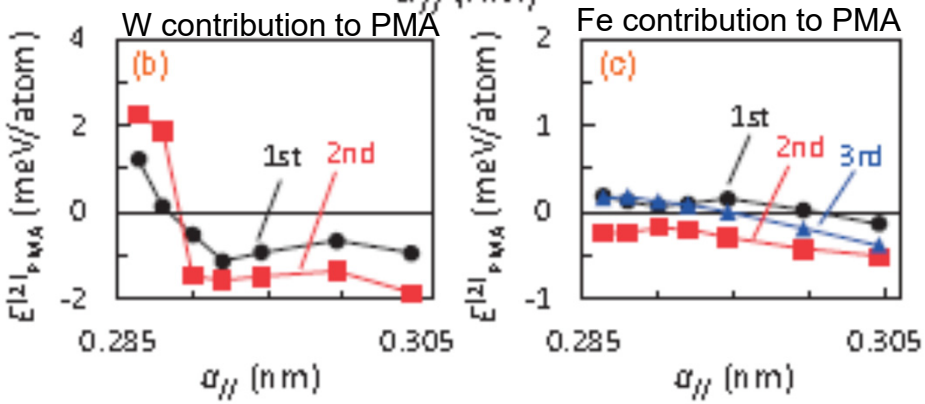

W insertion between Fe/MAO and Fe/MgO interfaces

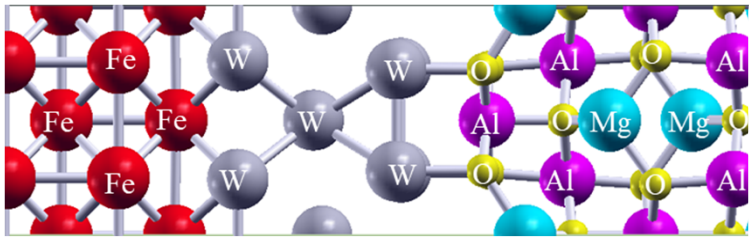

$a=a_{\mathrm{Fe}}$

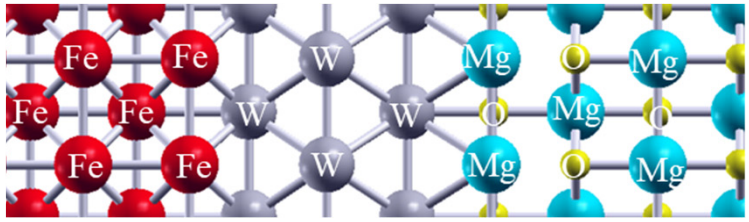

$a=a_{\mathrm{Fe}}$

$a=a_{\mathrm{MgO}}$

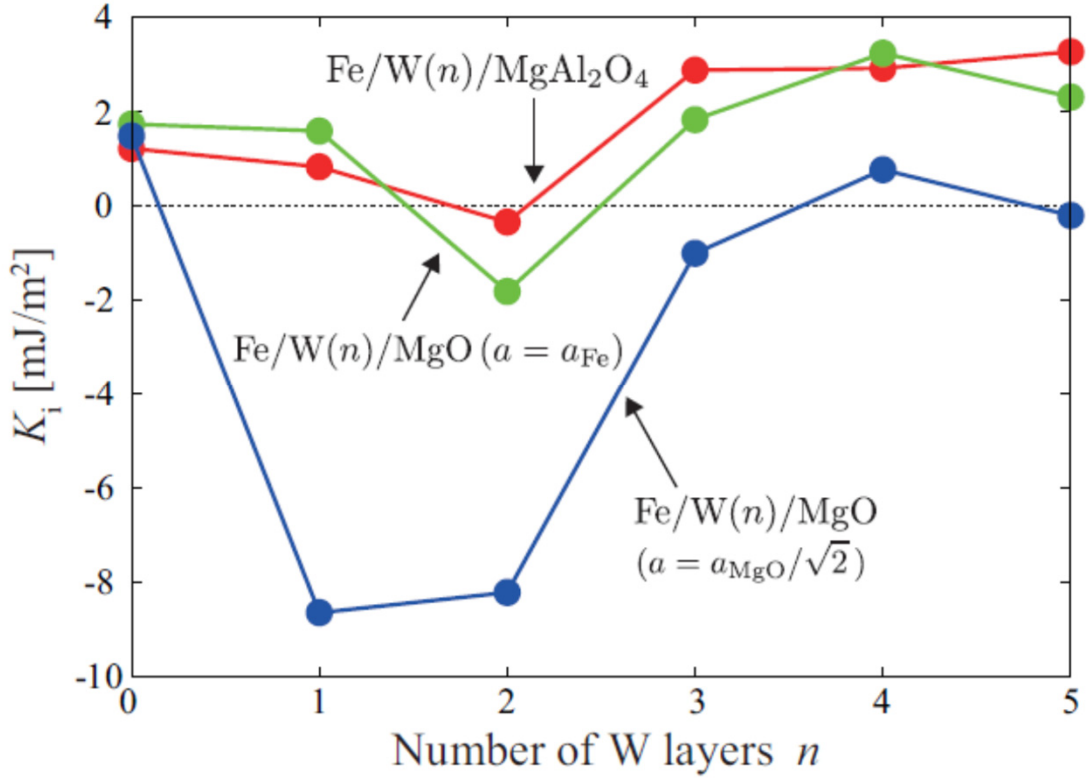

MAE contribution for each atom of Fe/W(3ML)/MgO(001) in $a=a_{Fe}$

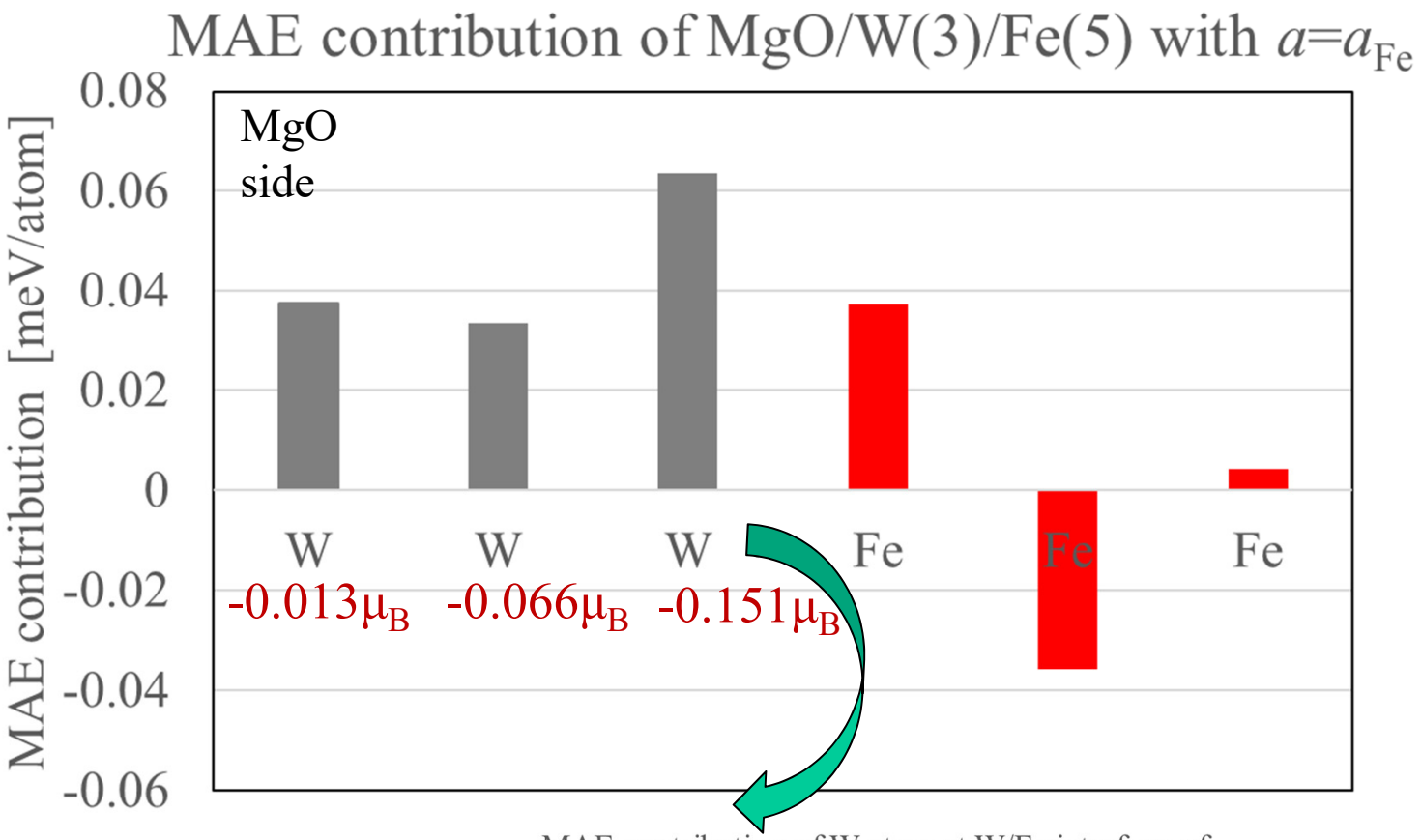

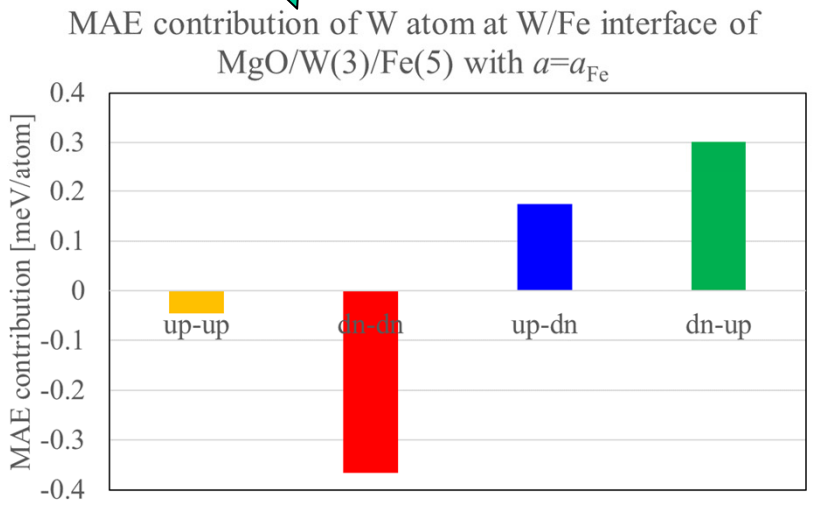

- Each W atom at W/Fe interface contribute to PMA.

- spin-flip term

Summary

	K_i (mJ/m^2)	$E_{demag}t$ (mJ/m^2)	$K_{eff}t=K_i-E_{demag}t$ (mJ/m^2)	$\Delta M_{orb,i}$ (μ_B/atom)	K_i (mJ/m^2) Experiments
Fe/$MgAl_2O_4$($a=a_{Fe}$)	1.192	-0.895	0.296	0.026	-
Fe/MgO($a=a_{MgO}/\sqrt{2}$)	1.617	-0.828	0.788	0.030	1.30 [1]
Fe/MgO($a=a_{Fe}$)	1.552	-0.908	0.643	0.020	0.98 [2]

- Fe/$MgAl_2O_4$(001) show PMA, which is slightly smaller than that of Fe/MgO(001).

- For Fe/MgO(001), not only spin conservation term $\Delta E_{\downarrow\Rightarrow\downarrow}$ but also spin-flip term $\Delta E_{\uparrow\Rightarrow\downarrow}$ contributes to PMA, resulting in larger PMA than that of Fe/$MgAl_2O_4$.

- 3ML W insertion between Fe and $MgAl_2O_4$ interfaces, Fe/W(3ML)/$MgAl_2O_4$(001), is promising to obtain large PMA more than 2mJ/m^2

Topics

0. Introduction on spintronics

1. First-Principles Study on magneto-crystalline anisotropy of Fe/MgO(001) and Fe/$MgAl_2O_4$(001)

K. Masuda and Y. Miura, PRB **98**, 224421 (2018).

2. First-Principles Study on magnetic damping of Fe/MgO(001)

Y. Miura, in preparation

3. First-Principles Study on Anisotropic Magneto-Peltier Effect

K. Masuda, K.-i. Uchida, R. Iguchi, Y. Miura PRB **99**, 104406 (2019)

Experiments electric field effects of PMA and magnetic damping

APPLIED PHYSICS LETTERS **105**, 052415 (2014)

Electric-field effects on magnetic anisotropy and damping constant in Ta/CoFeB/MgO investigated by ferromagnetic resonance

A. Okada,[1] S. Kanai,[1] M. Yamanouchi,[1,2] S. Ikeda,[1,2] F. Matsukura,[3,2,a)] and H. Ohno[1,2,3]
[1]*Laboratory for Nanoelectronics and Spintronics, Research Institute of Electrical Communication, Tohoku University, 2-1-1 Katahira, Aoba-ku, Sendai 980-8577, Japan*
[2]*Center for Spintronics Integrated Systems, Tohoku University, 2-1-1 Katahira, Aoba-ku, Sendai 980-8577, Japan*
[3]*WPI-Advanced Institute for Materials Research (WPI-AIMR), Tohoku University, 2-1-1 Katahira, Aoba-ku, Sendai 980-8577, Japan*

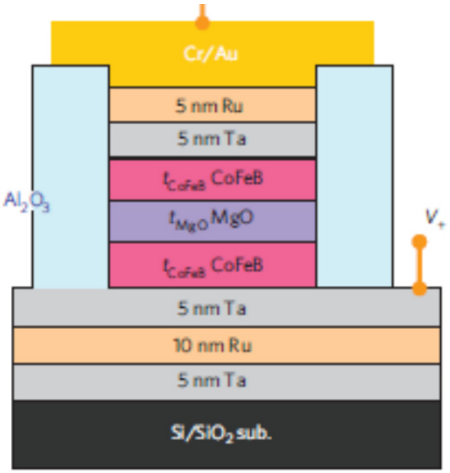

-21% of magnetic damping α is changed by 1V/nm EF for t=1.4nm

Magnetic anisotropy change by EF

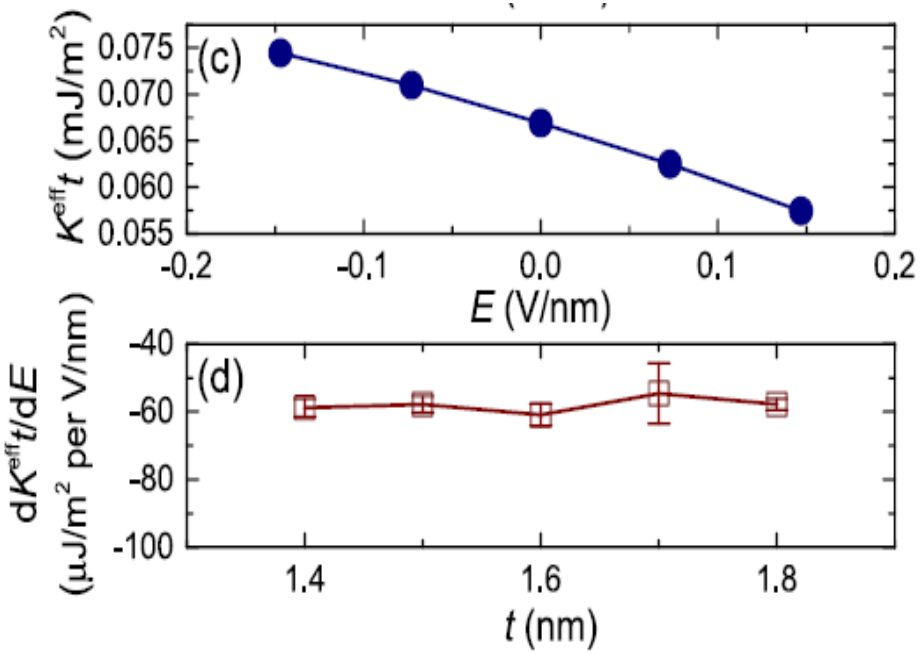

EF dependence is insensitive to thickness of FM layer

Magnetic damping change by EF

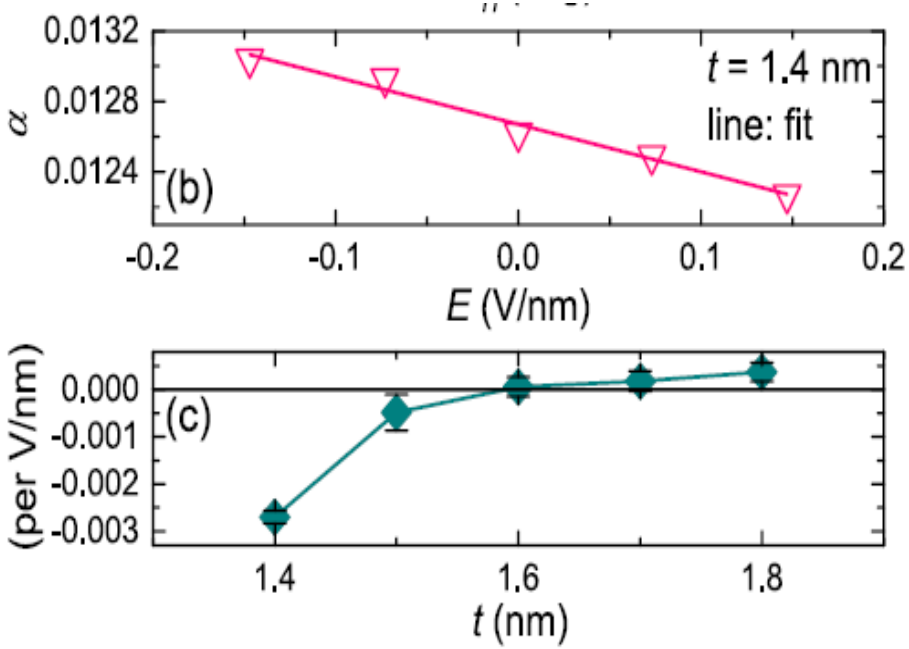

Large thickness dependence of FM layer

Kambersky's torque correlation model

V. Kambersky, Czechoslovak Journal of Physics B **26**, 1366 (1976).

Precession motion of local spin moment

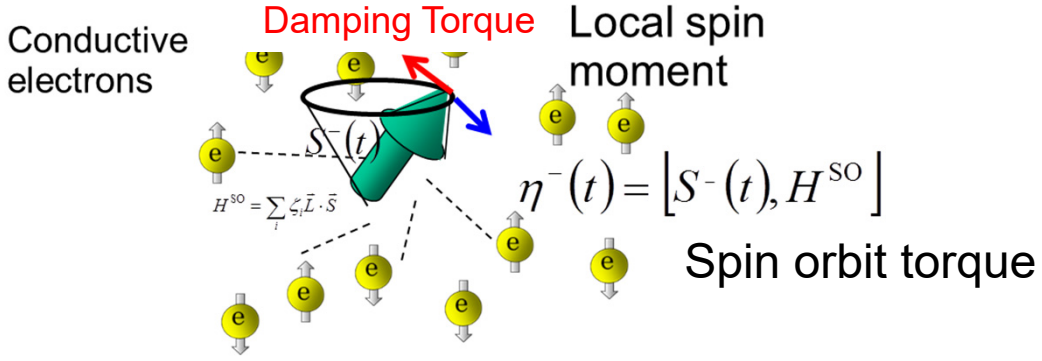

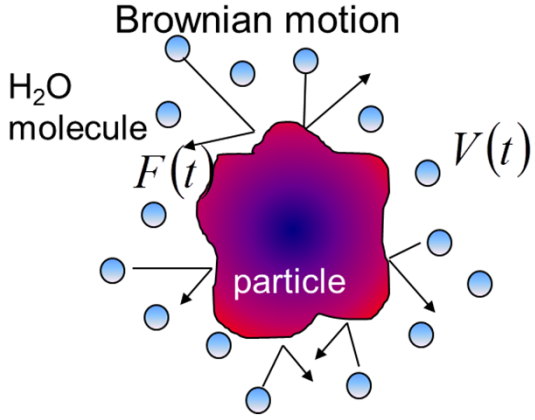

Generalized Langevin equation for magnetization dynamics

$$\frac{dS^-(t)}{dt}=\underbrace{-i\Omega S^-(t)}_{\text{Precession-tem}}\;\underbrace{-\;i\eta^-(t)}_{\text{Spin-torque term from SOI}}\;\underbrace{-\int_0^t P^{-1}\left\langle\left[\eta^-(t'),\eta^+\right]\right\rangle_0 S^-(t)dt'}_{\text{Damping-term}}$$

Magnetic susceptibility $\chi^+(\omega)=-\dfrac{\mu_0(g\mu_B)^2}{\hbar V}\dfrac{P}{\omega+i0-(\Omega-\Delta)-P^{-1}F(\omega+i0)}$

Green function of Torque operator $F(\omega+i0)=-i\int_{-\infty}^{\infty}\left\langle\left[\eta^-(t),\eta^+\right]\right\rangle_0\theta(t)e^{i(\omega+i0)t}dt$

Magnetic susceptibility from LLG equation $\chi^+(\omega)=-\dfrac{\gamma M_s}{\omega-\gamma H_{eff}+i\alpha\omega}$

Magnetic damping constant (comparing macroscopic formula) $\alpha=-\lim_{\omega\to 0}\dfrac{\gamma}{\hbar\mu_0 V M_S}\mathrm{Im}\left[\dfrac{1}{\omega}F(\omega+i0)\right]$

Purpose of this work

If PMA and magnetic damping can be simultaneously reduced by applied voltage, we can drastically reduce power consumption and write error rate in magnetization reversal of MRAM.

Voltage dependence of magnetic damping is hardly investigated.

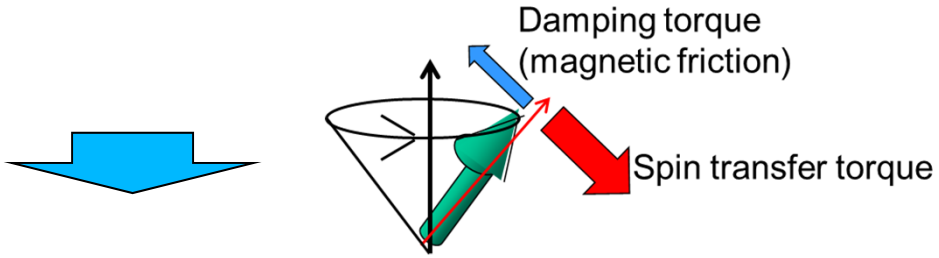

This work investigates the voltage dependence of magnetic damping and magnetic anisotropy of Fe/MgO interface based on the first-principles calculation.

Origin of Magnetic Damping α

- Electronic system
- Phonon
- Atomic disorder
- Other extrinsic factors

First-principles calculation of damping constant

V. Kambersky, Czechoslovak Journal of Physics B **26**, 1366 (1976).

$$\alpha = \frac{g^2 \mu_0 \mu_B^2}{\pi \hbar V \gamma M_S} \sum_{\vec{k}} \sum_{nm} \left| \Gamma_{nm}^{-}(\vec{k}) \right|^2 \frac{\delta}{\left(E_F - E_{n\vec{k}}\right)^2 + \delta^2} \frac{\delta}{\left(E_F - E_{m\vec{k}}\right)^2 + \delta^2}$$

Eigenstates at each k-point and band

$$\gamma = \mu_0 g \mu_B / \hbar$$

Matrix elements of torque operator

$$\Gamma_{nm}^{-}(\vec{k}) = \left\langle n, \vec{k} \left| \zeta \left[S^{-}, H^{SO} \right] \right| m, \vec{k} \right\rangle$$

$H_{SO} = \xi \vec{L} \cdot \vec{S}$ Spin-orbit interaction

$$\left| m, \vec{k} \right\rangle = \sum_{i,\mu,\sigma} c_{i\mu}^{\vec{k}m\sigma} \left| i\mu \right\rangle$$

matrix elements of torque operator based on the local atomic orbital

VASP code

Bulk-Fe

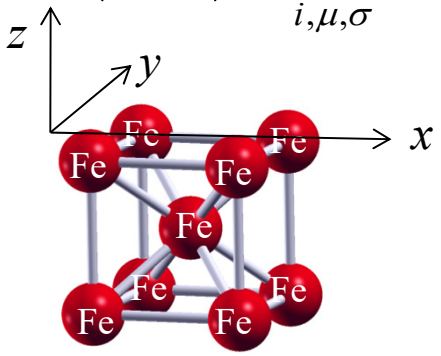

α=0.0011 (this work)

α=0.0013 (by Gilmore)

K. Gilmore, PRL **99,** 027204 (2007)

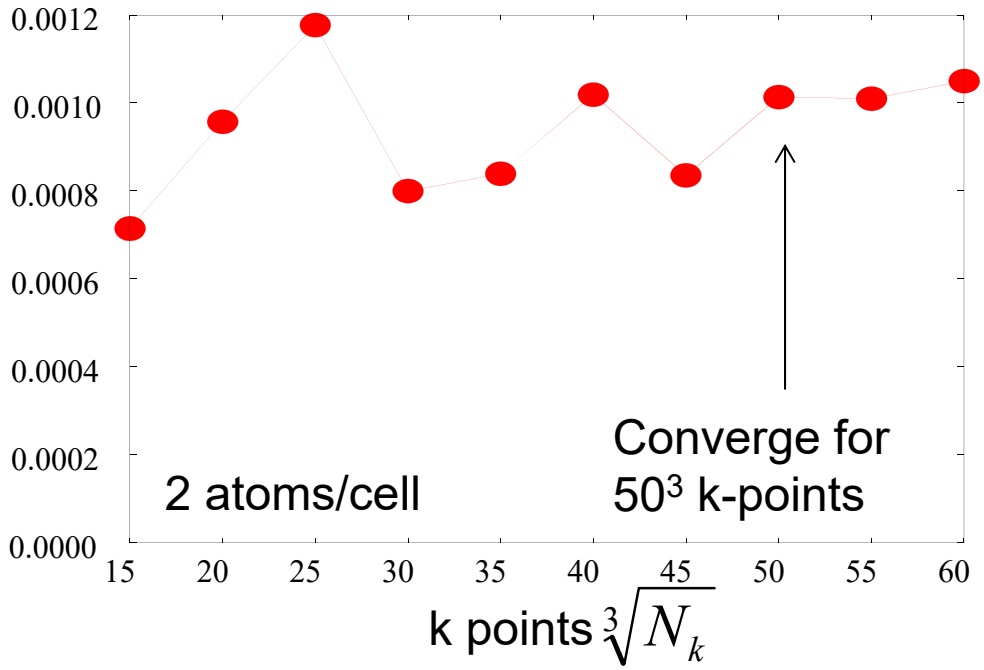

⇒For Fe/MgO(001) interface, I considered 50x50 k-points.

Potential and charge for model system

Dipole correction⇒ G. Makov and M. C. Payne, PRB **51**, 4014 (1995).

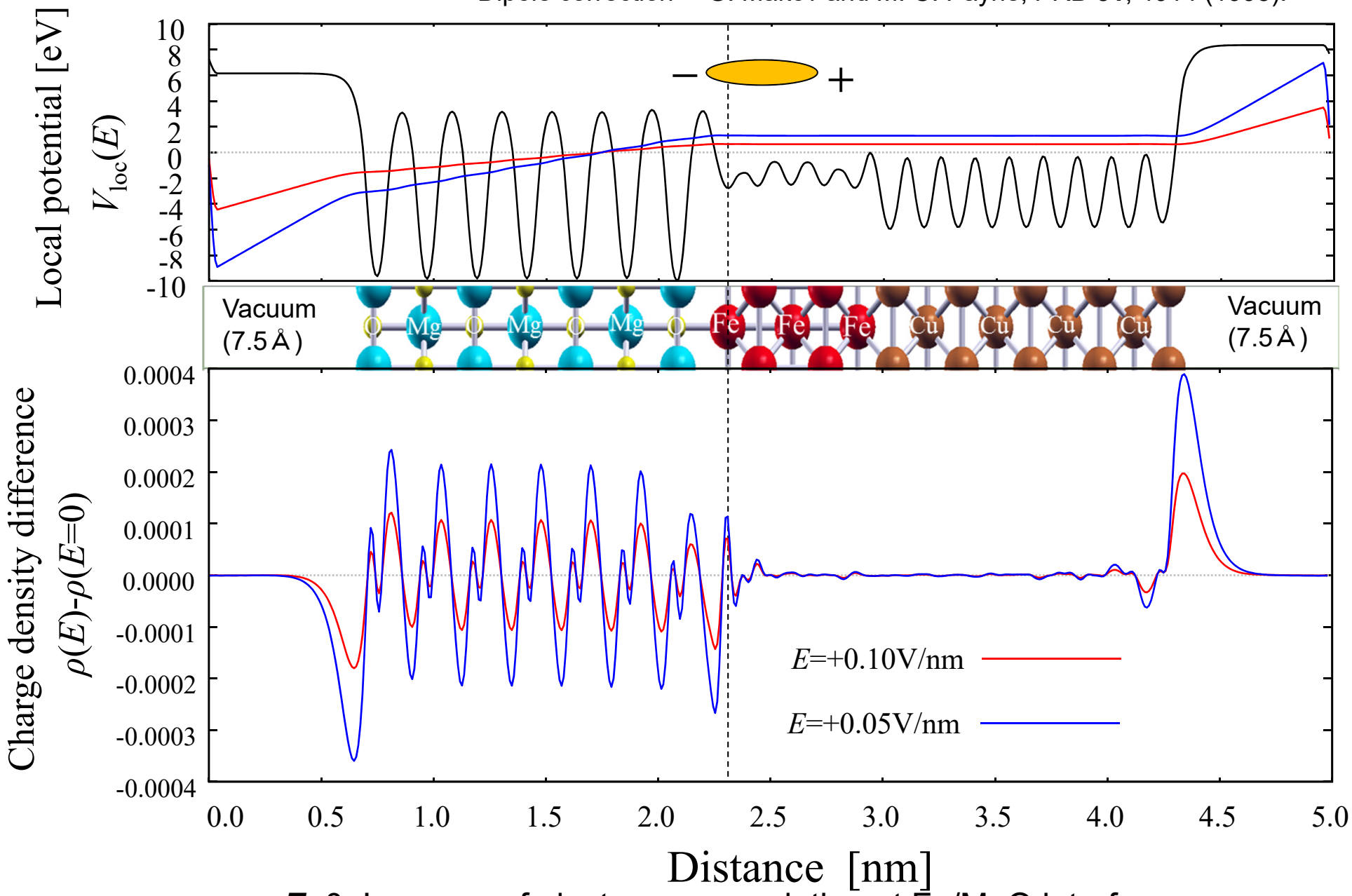

E>0 :Increase of electron accumulation at Fe/MgO interface

E<0 :Decrease of electron accumulation at Fe/MgO interface

Voltage dependence of PMA and damping α of Fe surface and Fe/MgO interface

Fe(001) surface

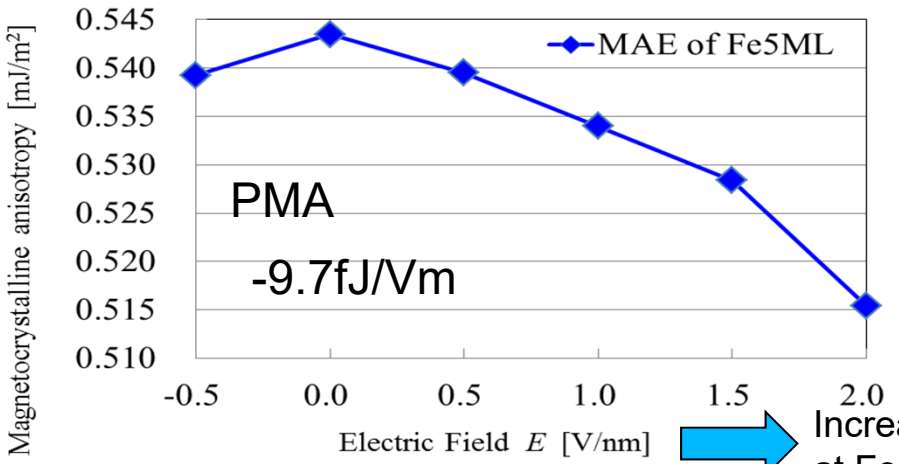

Increase of electron at Fe surface

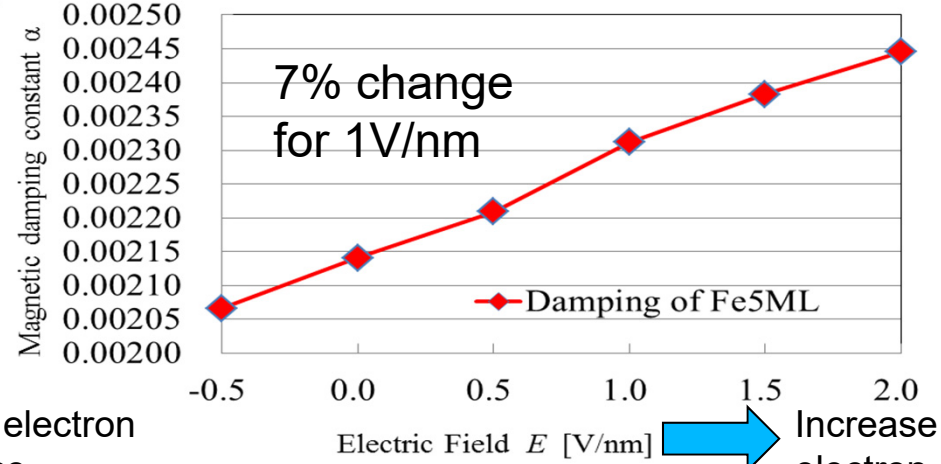

Increase of electron at Fe surface

C. G. Duan, *et al*., PRL **101**, 137201 (2008).

Fe/MgO(001) interface

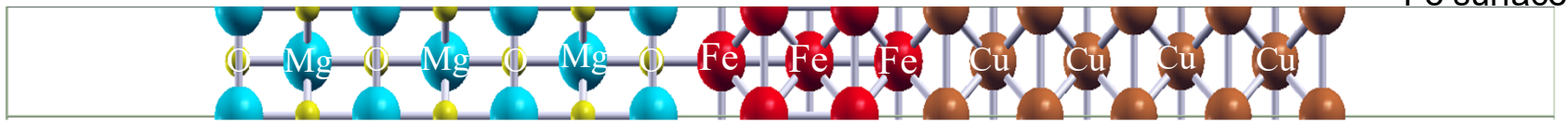

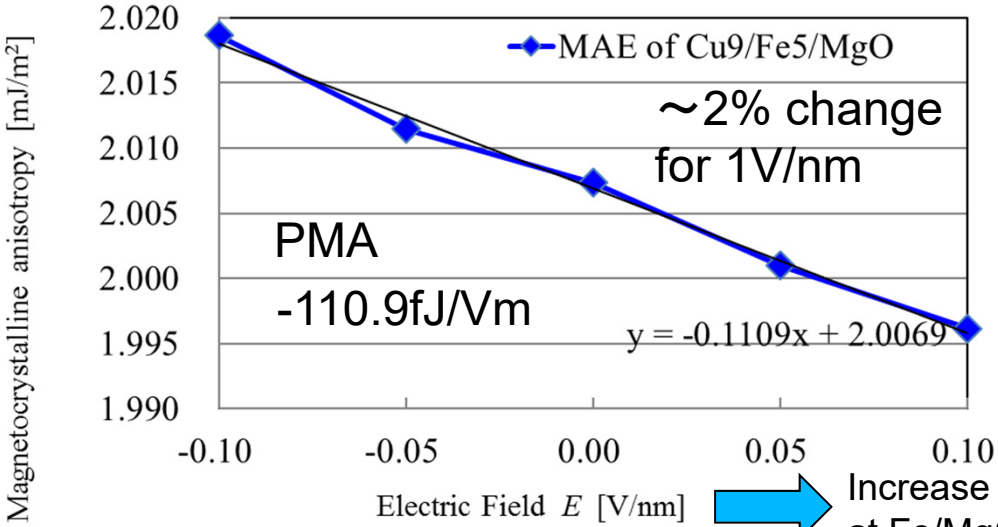

Increase of electron at Fe/MgO interface

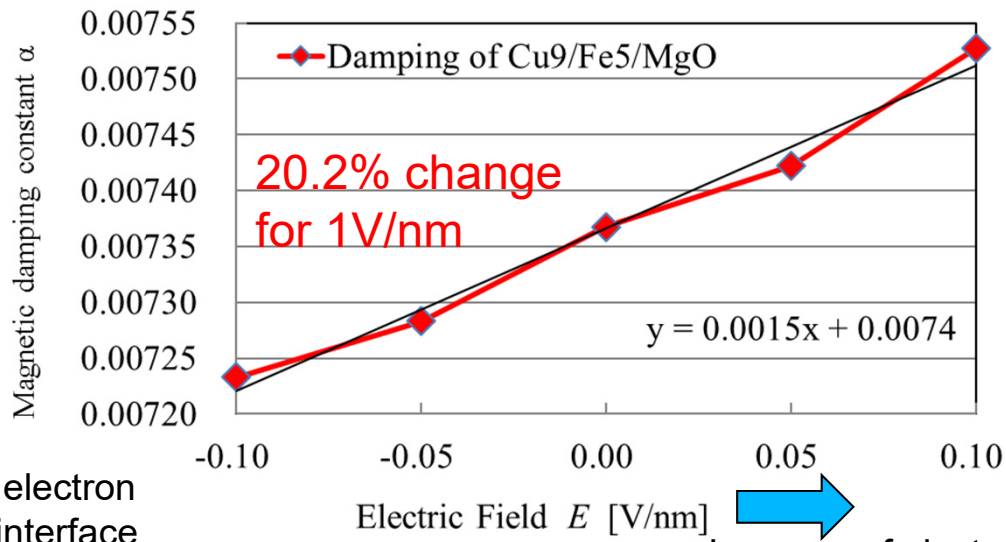

Increase of electron at Fe/MgO interface

Decomposition of magnetic damping α

Torque operator $\Gamma^- = \left[S^-, H^{SO}\right] = \zeta\left(S^z L^- - S^- L^z\right)$

Spin conservation (Orbital deexcitation) term

$\left\langle u^\sigma \left| L^- \right| o^\sigma \right\rangle$

The matrix elements are non-zero for atomic orbitals between different magnetic quantum number, such as d(yz,zx)-d(z^2), d(yz,zx)-d(x^2-y^2), d(yz,zx)-d(xy)

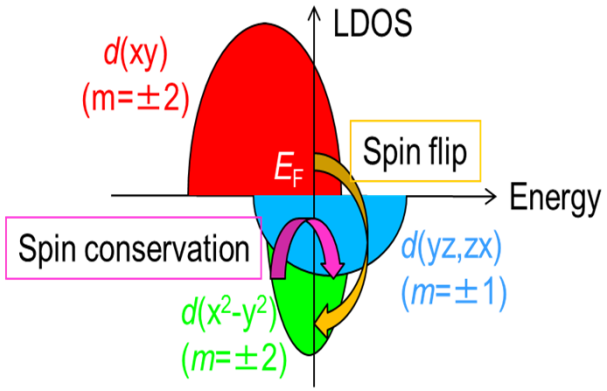

Spin flip (Orbital conservation) term

$\left\langle u^{-\sigma} \left| L_Z \right| o^\sigma \right\rangle$

The matrix elements are non-zero for atomic orbitals between same magnetic quantum number, such as d(yz)-d(zx),d(x^2-y^2)-d(xy)

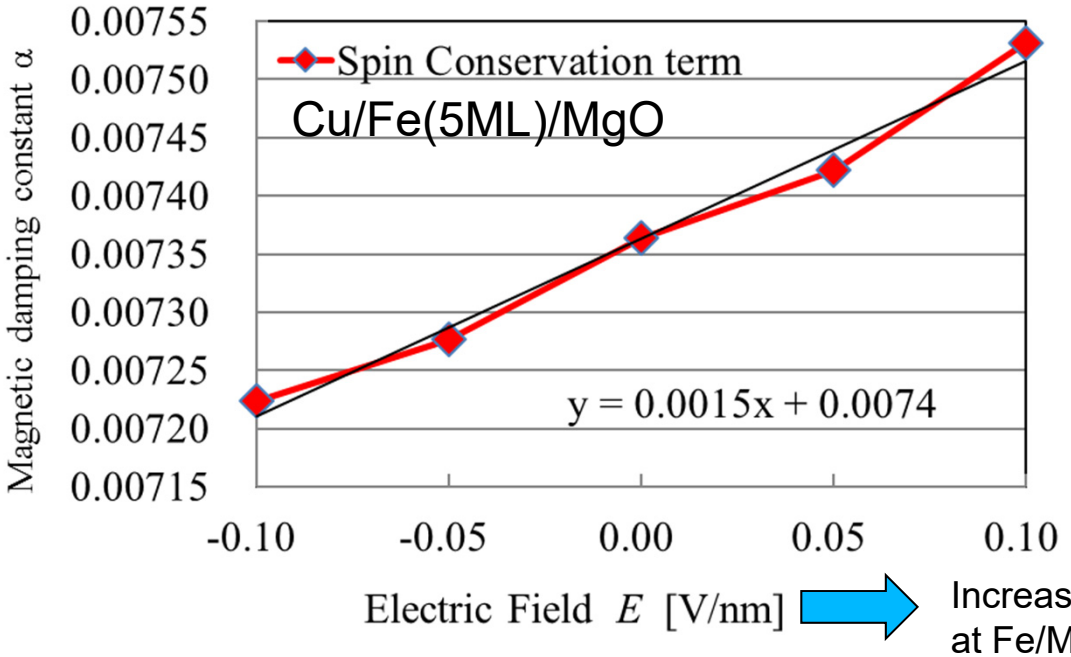

Increase of electron at Fe/MgO interface

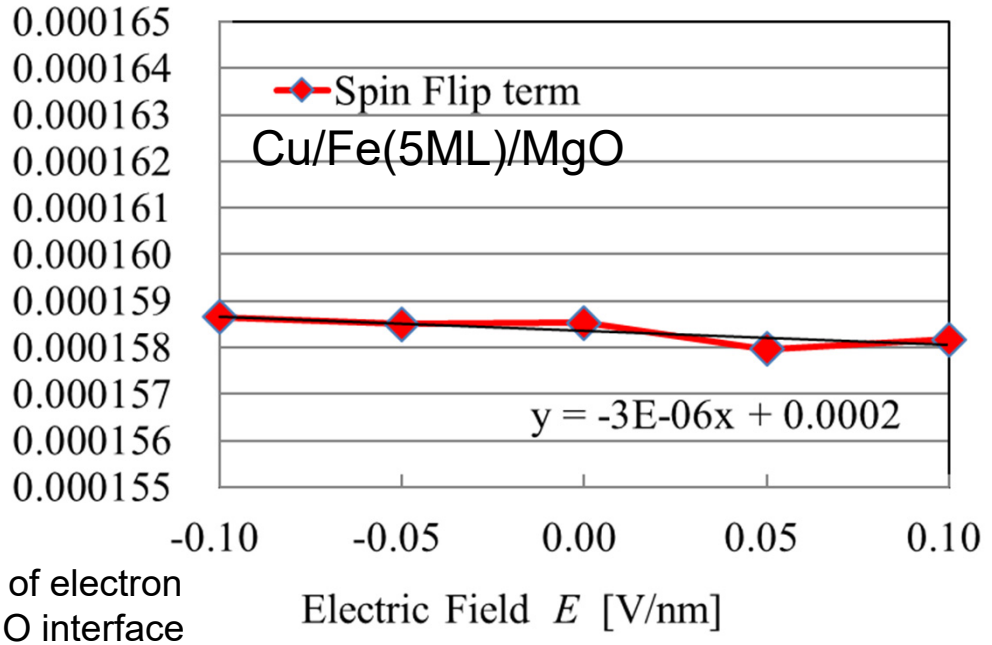

Origin of electric filed dependence

Fe/MgO(001) interface

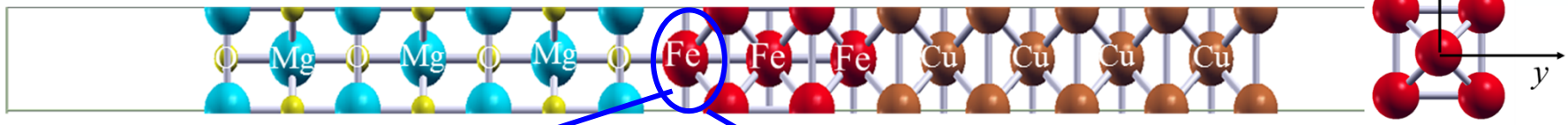

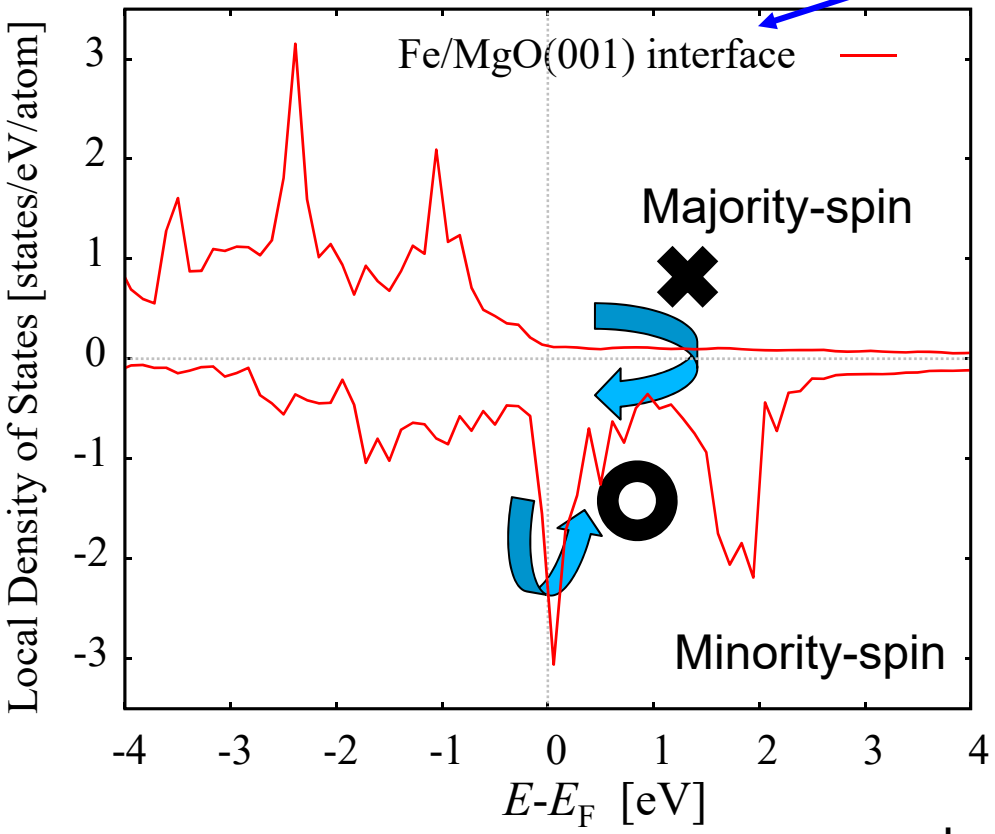

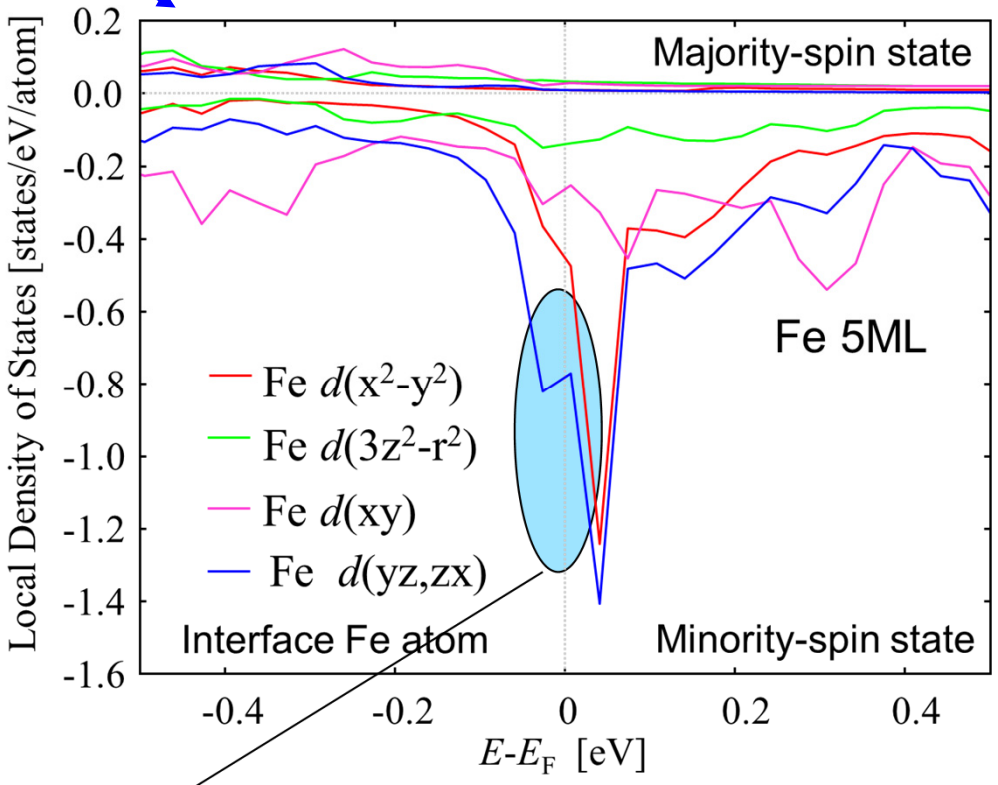

Large matrix element of $\langle d(x^2-y^2)|L^-|d(yz,zx)\rangle$

Increase damping with increasing EF

Second order perturbation of SOI

D. Wang, et al., PRB **47**, 14932 (1993).

$$E_{\mathrm{PMA}} \propto (\xi)^2 \sum_{o,u,k} \frac{\left|\langle o,k,\downarrow|L_z|u,k,\downarrow\rangle\right|^2 - \left|\langle o,k,\downarrow|L_x|u,k,\downarrow\rangle\right|^2}{\varepsilon^{\downarrow}_{u,k} - \varepsilon^{\downarrow}_{o,k}}$$

$$L_x = \tfrac{1}{2}\left(L^- + L^+\right)$$

The $\langle d(x^2\text{-}y^2)|L^-|d(yz)\rangle$ increase the damping, but decrease the PMA.⇒opposite EF dependence

Summary of the second topic

First principles study on voltage control of magnetic anisotropy (VCMA) and magnetic damping in Fe/MgO interface

- For Fe/MgO(001) surface, the magnetic damping increases with increasing the electron accumulation at interface (positive EF).

  (20% of damping constant α can be changed by EF=1[V/nm] for Fe/MgO(001))

- It is opposite to that of PMA (perpendicular magnetic anisotropy).

- The voltage dependence of magnetic damping of Fe/MgO(001) can be attributed to the spin conservation term.

Topics

0. Introduction on spintronics

1. First-Principles Study on magneto-crystalline anisotropy of Fe/MgO(001) and Fe/$MgAl_2O_4$(001)

K. Masuda and Y. Miura, PRB **98**, 224421 (2018).

2. First-Principles Study on magnetic damping of Fe/MgO(001)

Y. Miura, in preparation

3. First-Principles Study on Anisotropic Magneto-Peltier Effect

K. Masuda, K.-i. Uchida, R. Iguchi, Y. Miura PRB **99**, 104406 (2019)

Introduction

Magnetoresistance devices

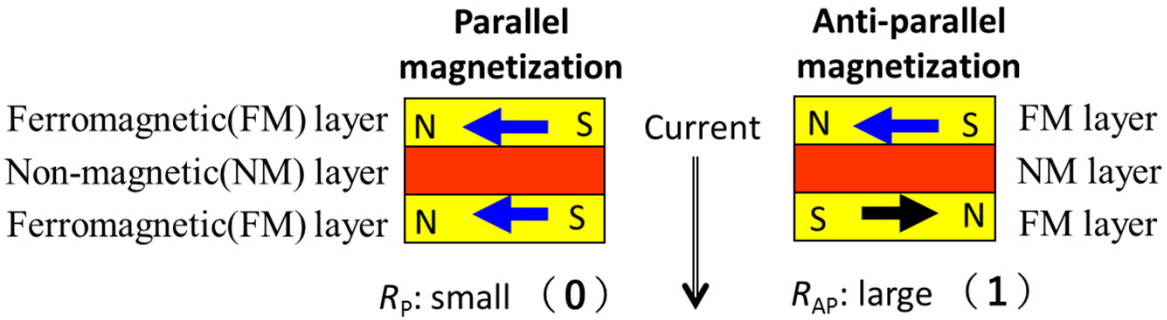

Magnetoresistance (MR)

$$\text{MR ratio} = \frac{R_{AP} - R_P}{R_{AP}}$$

MRAM

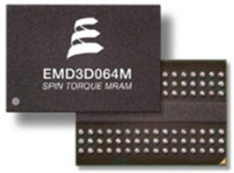

Spin Torque Oscillator

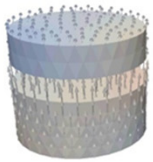

Read-Out-Head of HDD

Ultra-sensitive magnetic censer

Earth's magnetic field censer

current censer for car

biomagnetic censer

Thermal management of spintronics devices

- Thermal spin torque transfer

  X. Jia *et al.*, PRL. **107**, 176603 (2011).

- Thermal readout of MRAM

  B. Geisler, P. Kratzer PRB. **92**, 144418 (2015).

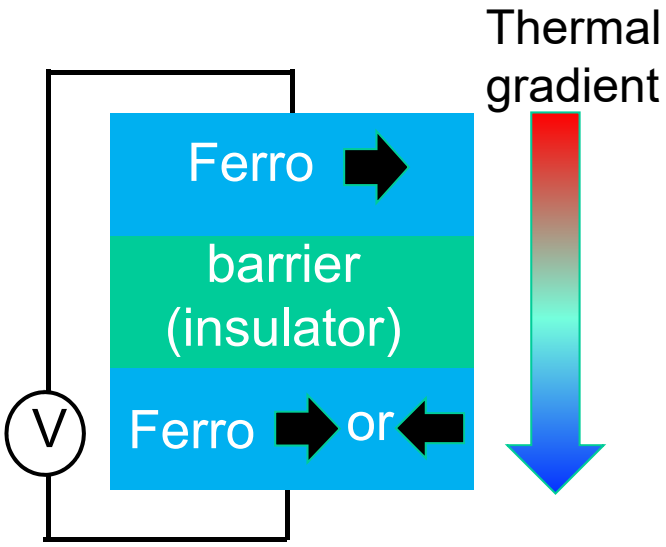

Thermal managements in MTJs

TMR ratio of MTJs with Co_2MnSi(CMS)-MgO

S. Tsunegi, *et al.*, APL 93 (2008) 112506.

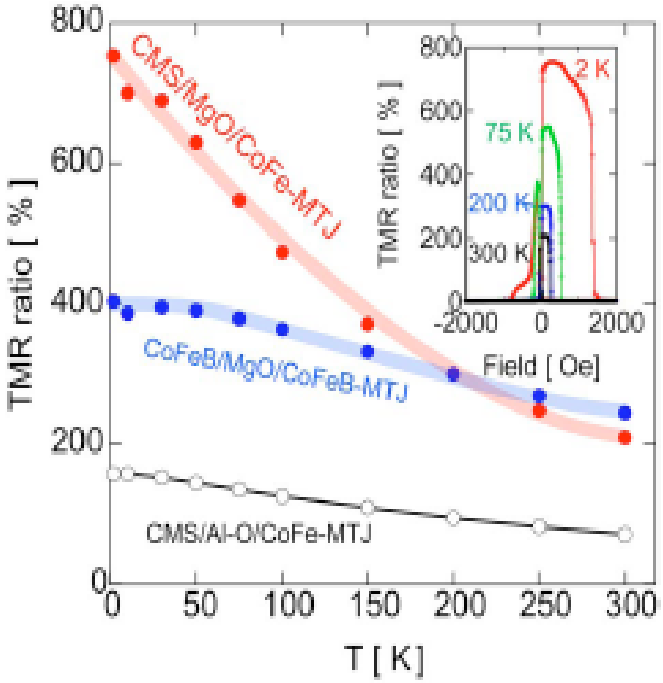

Problem: Reduction of the TMR ratio at room temperature

in spite of high curie temperature ～1000K

・Self-cooling of MTJs by magneto-Peltier effect

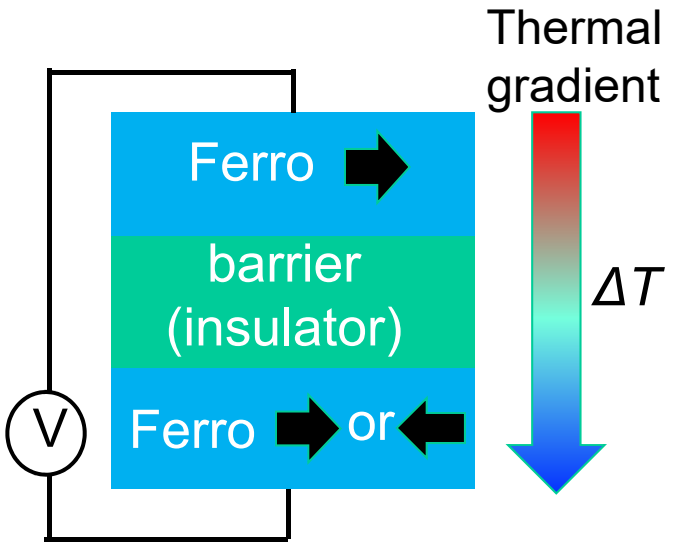

Observation of Anisotropic Magneto-Peltier Effects (AMPE)

K. Uchida, *et al.,* Nature, 558 (2018) 95.

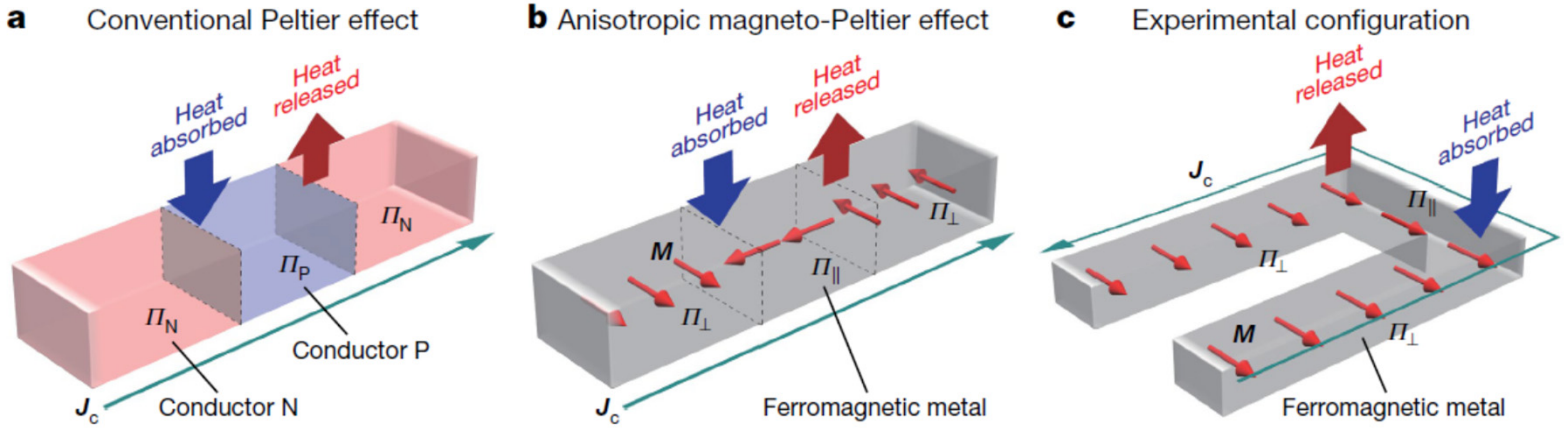

Fig. 1 | Conventional Peltier and anisotropic magneto-Peltier effects. **a**, Schematic of the conventional Peltier effect in a junction comprising two conductors P and N. When a charge current J_c is applied to the junction, the Peltier effect induces heat absorption or release at the P|N interface owing to the difference between the Peltier coefficient of P, Π_P, and that of N, Π_N. **b**, Schematic of the anisotropic magneto-Peltier effect (AMPE) in a ferromagnetic metal. When J_c is applied to the ferromagnet with the magnetization vector $\boldsymbol{M}$, the AMPE induces heat absorption or release even in the absence of junctions, because of the difference between the Peltier coefficient for the region with $\boldsymbol{M} \perp J_c$, $\Pi_\perp$, and that with $\boldsymbol{M} \parallel J_c$, $\Pi_\parallel$. **c**, Experimental configuration for measuring the AMPE in a U-shaped ferromagnet.

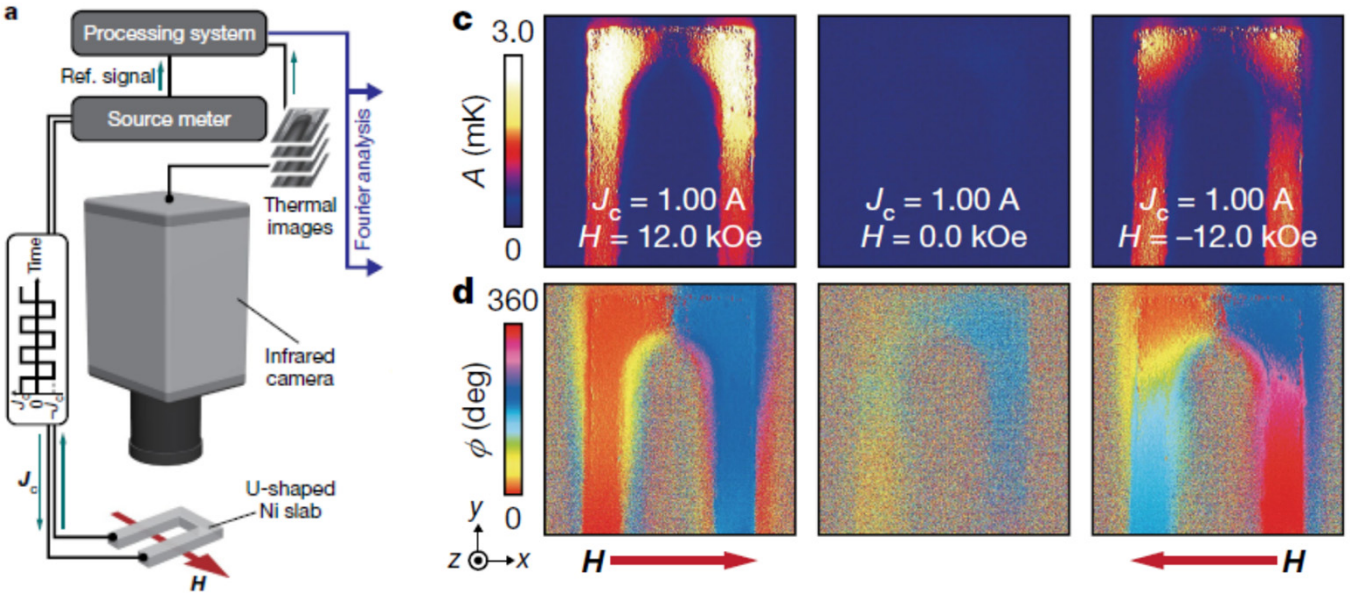

Large AMPE was observed for Ni, but not for Fe.

First-principles calculations of Seebeck and Peltier coefficient

Group velocity

$$v_\alpha\left(n,\vec{k}\right)=\frac{1}{\hbar}\frac{\partial\varepsilon\left(n,\vec{k}\right)}{\partial k_\alpha}$$

（k-vector derivative of band dispersion ）

（WIEN2k+BoltzTraP code）

$$e^2K_0=e^2\tau\int D(\varepsilon)\left(-\frac{\partial f_0}{\partial\varepsilon}\right)(\varepsilon-\mu)^0 d\varepsilon$$

$$e^2K_1=e^2\tau\int D(\varepsilon)\left(-\frac{\partial f_0}{\partial\varepsilon}\right)(\varepsilon-\mu)^1 d\varepsilon$$

Seebeck Coefficient $\alpha=-\frac{K_1}{eK_0T}$

Peltier coefficient $\pi=-\frac{K_1}{eK_0}=\alpha T$

Anisotropic magneto-Seebeck effect

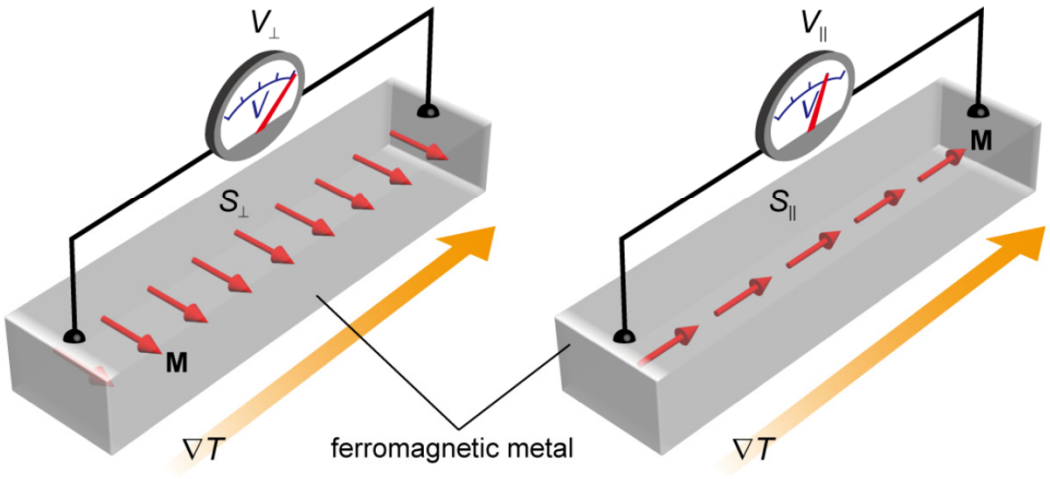

Anisotropic magneto-Peltier effect

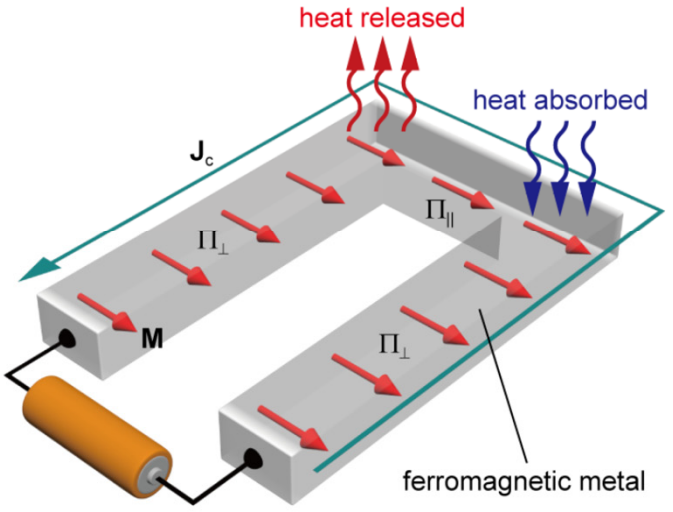

Spin-orbit interaction (SOI) and anisotropic magneto-Peltier effect (AMPE)

Spin-orbit interaction

Nuclear

Electron spin

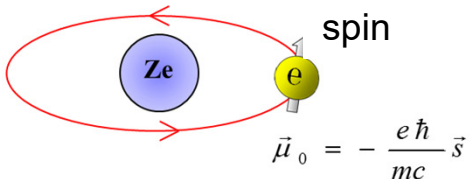

$$\vec{\mu}_0 = -\frac{e\hbar}{mc}\vec{s}$$

Magnetic field by electron motion

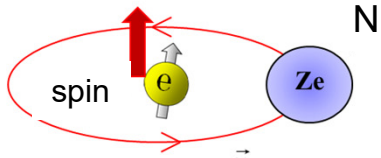

$$\vec{H}_{eff} = \frac{\vec{v}}{c} \times \vec{E}$$

Interaction between electron spin and magnetic field by the orbital motion

$$H_{sp} = -\vec{\mu}_0 \cdot \vec{H}_{eff}$$

$$H_{sp} = \zeta \vec{l} \cdot \vec{s}$$

Spin-orbit constant $\zeta = \frac{\hbar}{2mc^2}\frac{1}{r}\frac{dV}{dr}$

⇒ Coupling between spin (magnetization direction) and orbital (crystal axis)

⇒ Anisotropic band dispersion

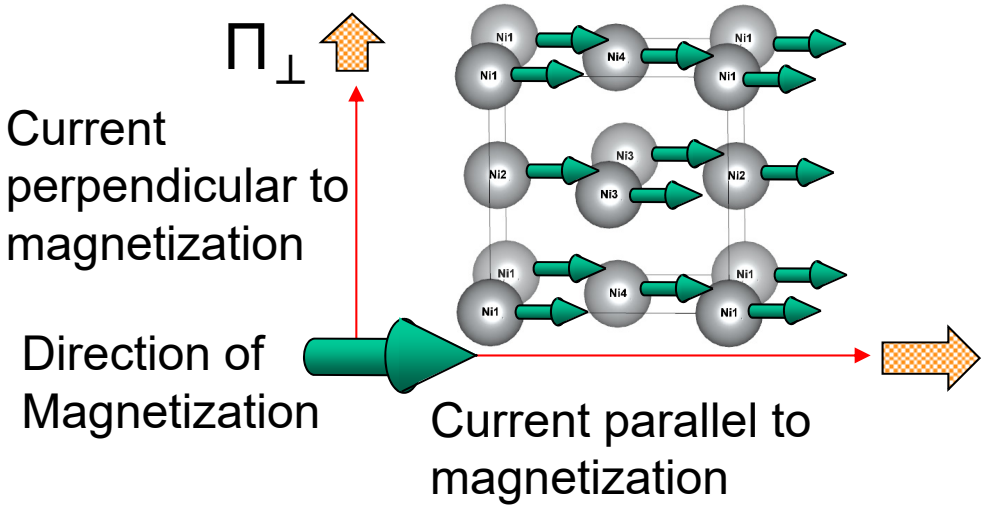

Without SOI

Peltier coefficient : $\Pi_\perp = \Pi_{//}$

With SOI

Peltier coefficient : $\Pi_\perp \neq \Pi_{//}$

Anisotropic magneto-Peltier effects (AMPE) of Fe,Co,Ni

bcc-Fe (2atoms/u.c.)

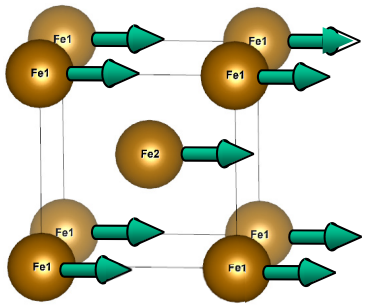

fcc-Ni (4atoms/u.c.)

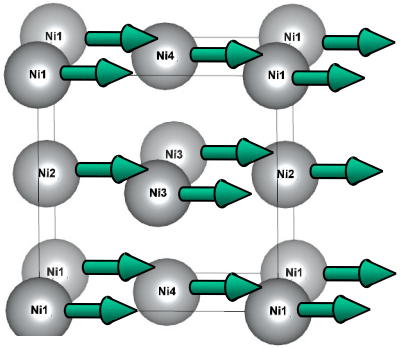

$S_{//}$

$S_{\perp}$

Definition of AMPE

$$\Delta\Pi / |\Pi_{\perp}| = (\Pi_{\perp} - \Pi_{//}) / |\Pi_{\perp}|$$

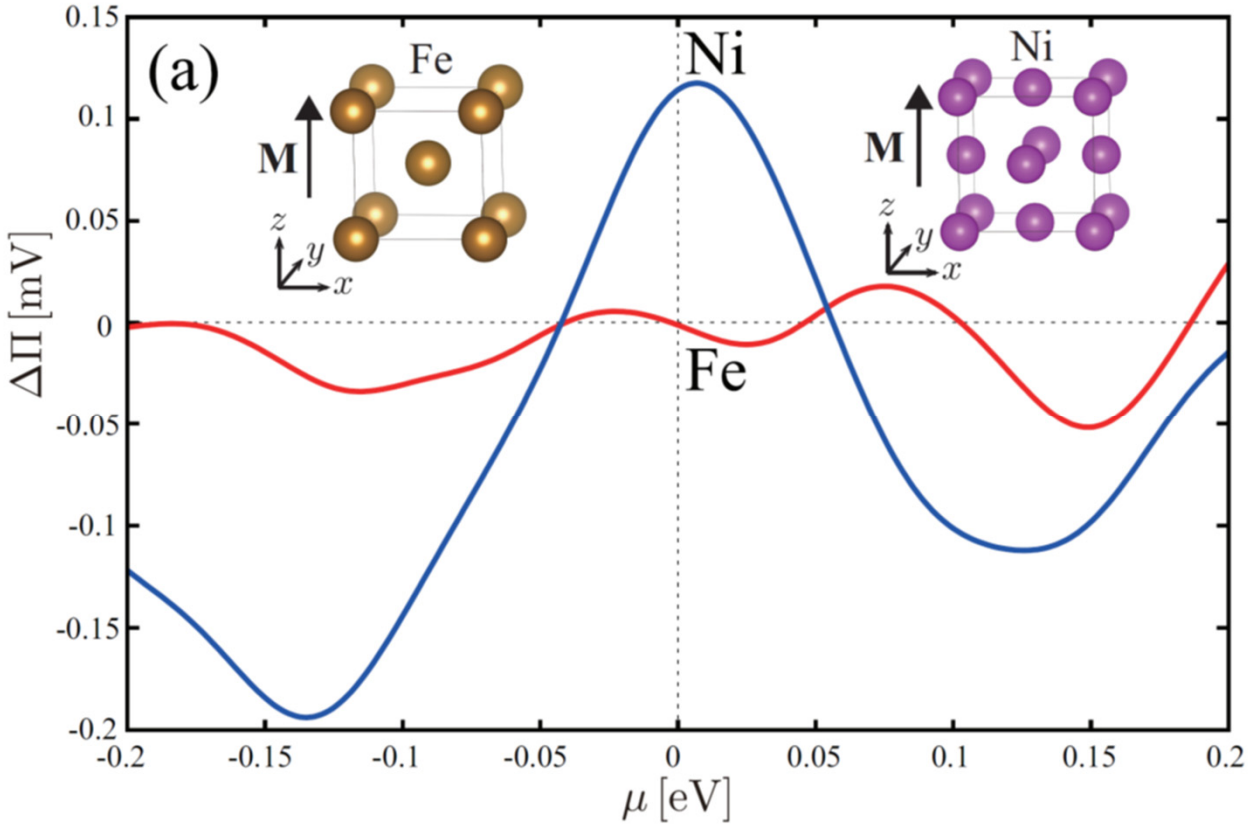

Comparison of band dispersion of Fe, Ni

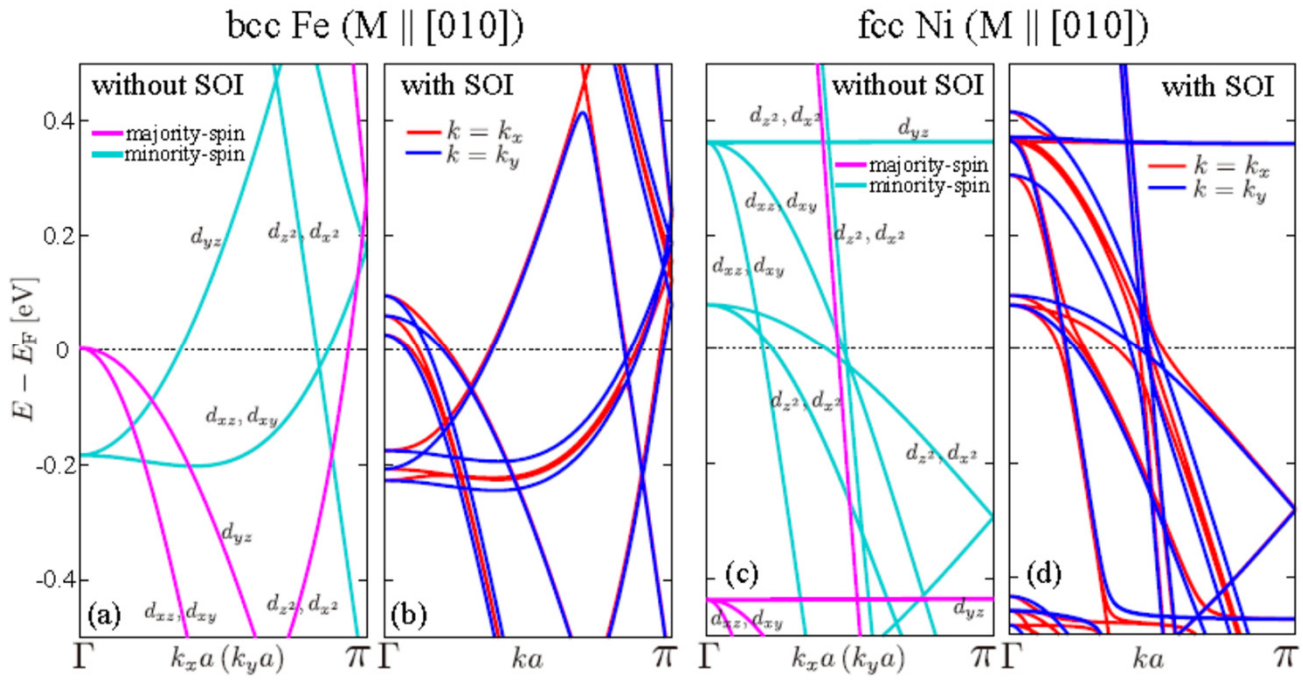

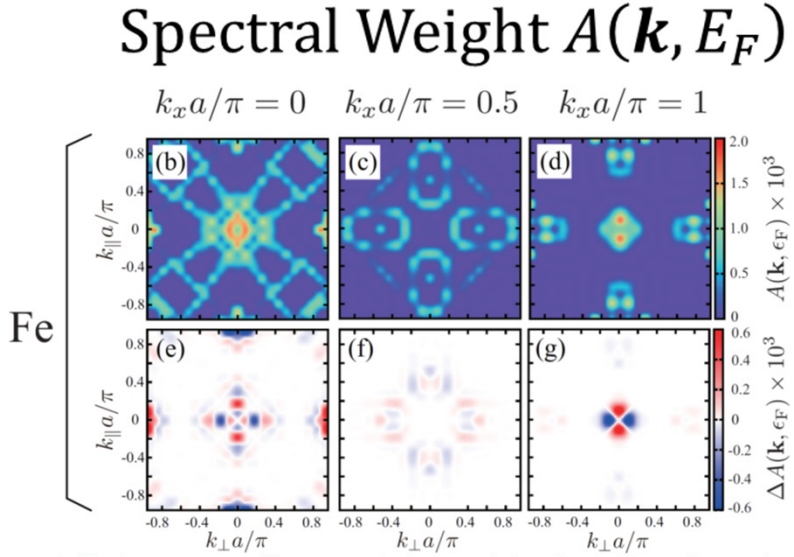

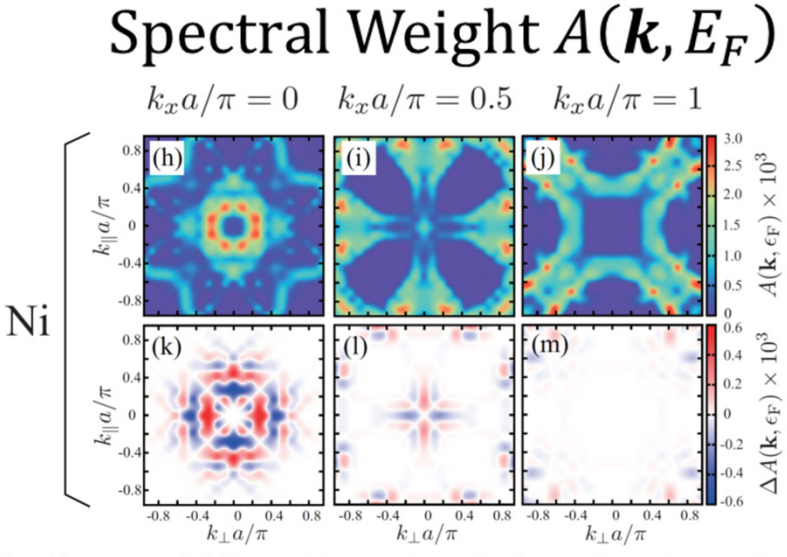

Ni: Large *d*(*xz*,*xy*)-band hybridization between Majority- and Minority-spin states due to spin-orbit⇒Large AMPE(*ΔΠ*)

Mechanism of AMPE in Fe, Ni

$$\xi\vec{L}\cdot\vec{S} = \frac{\xi}{2}\underbrace{(L^{+}S^{-} + L^{-}S^{+})}_{\text{Spin-flip term}} + \underbrace{L^{z}S^{z}}_{\text{Spin-conserving term}}$$

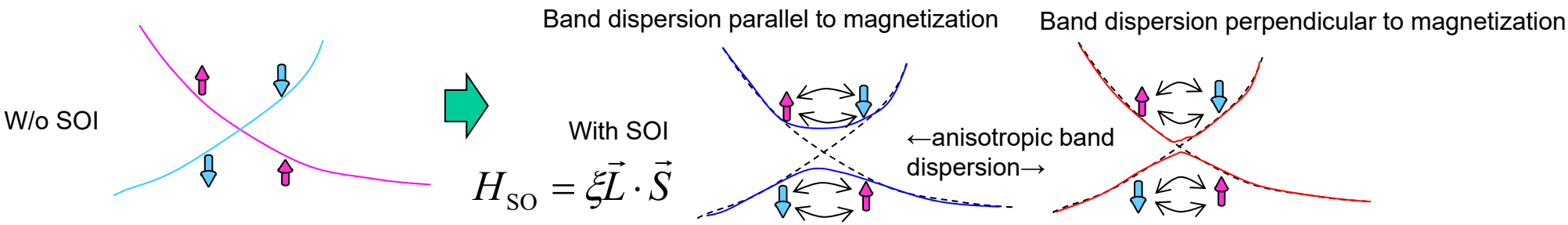

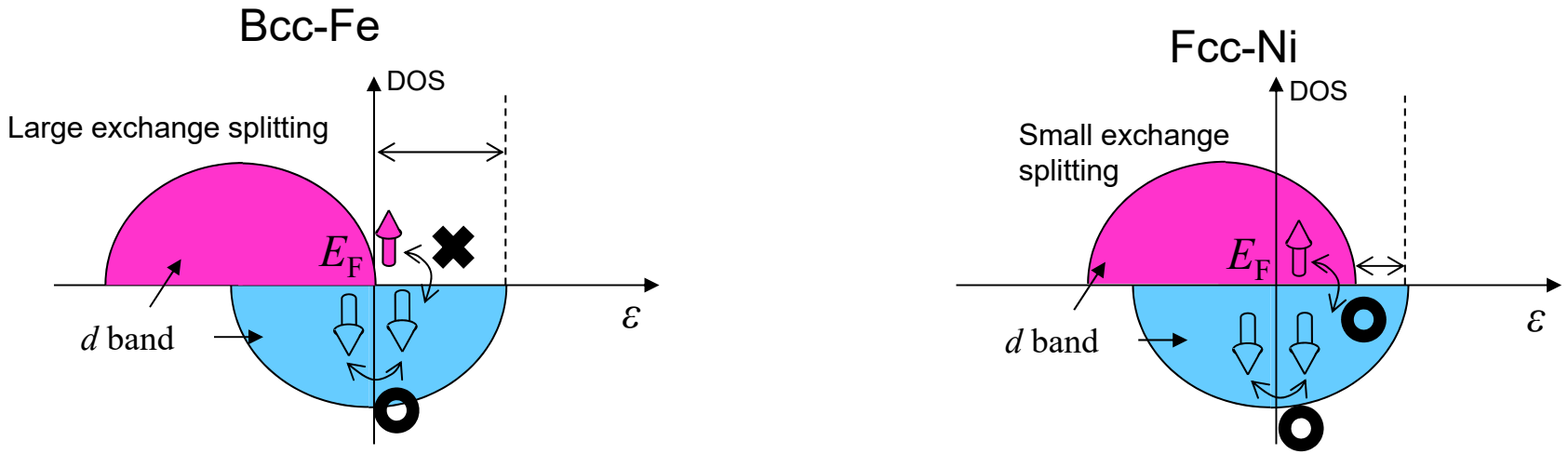

d-Band hybridization between majority- and minority-spin states due to SOI is important for large AMPE.
To this end, ferromagnetic materials with small exchange splitting such as Ni is more favorable for large AMPE.

Prediction of new materials with huge AMPE

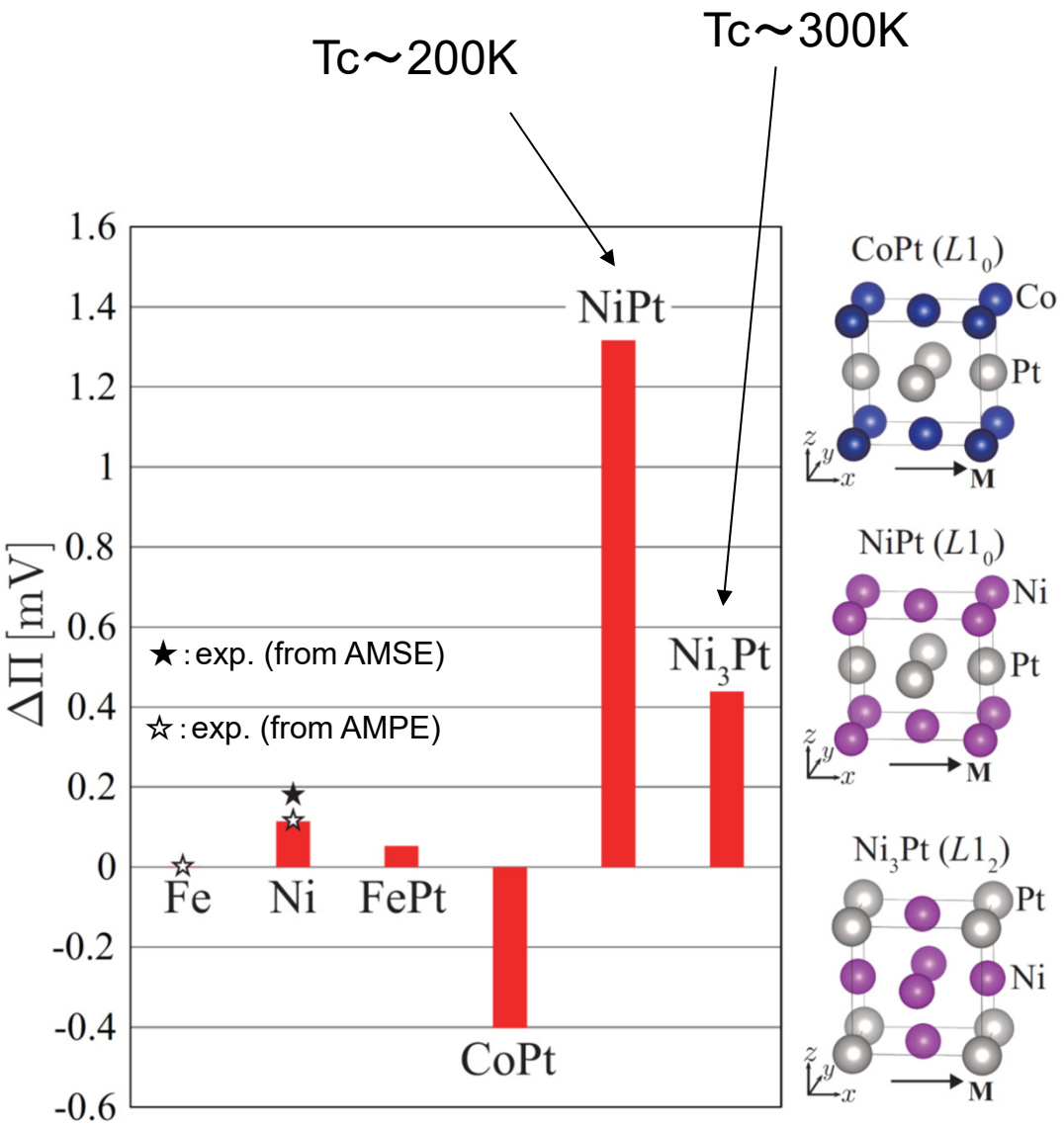

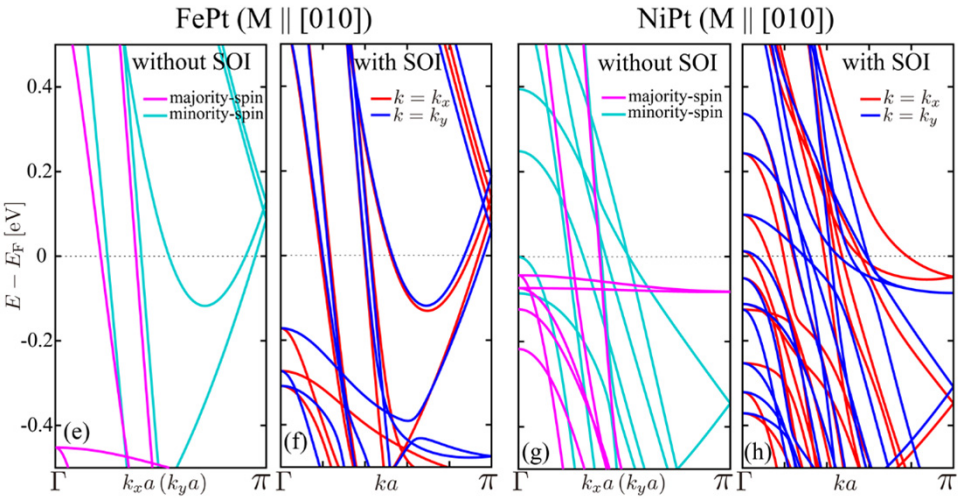

FePt 3.30μ_B/cell NiPt 1.06μ_B/cell

Smaller exchange splitting of NiPt than FePt

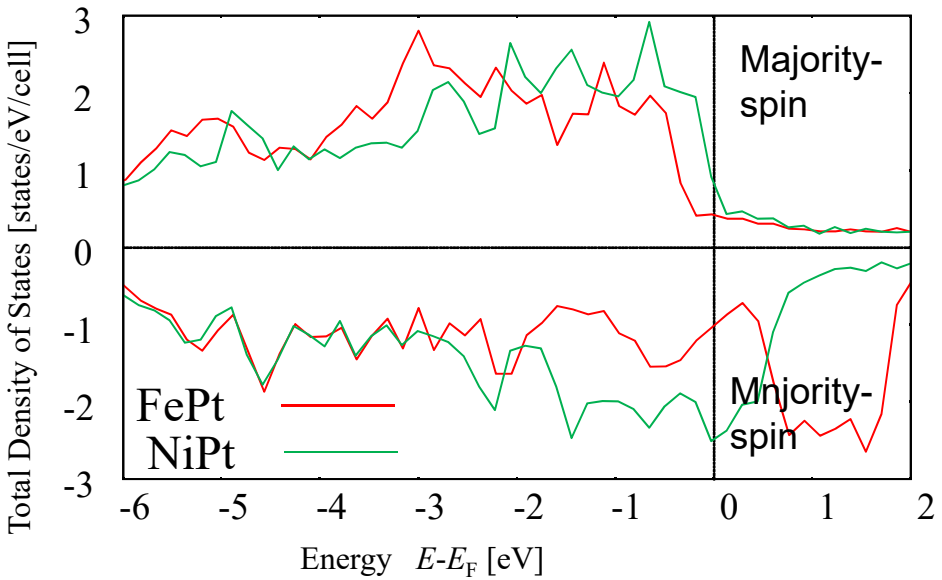

Summary of the third topic

・In first-principles calculations, AMPE is Fe<Co<Ni, and FePt<<NiPt<Ni_3Pt.

・Hybridization of Majority-spin and Minority-spin d-band around the Fermi level is more important for large AMPE.

Summary of this talk

MRAM

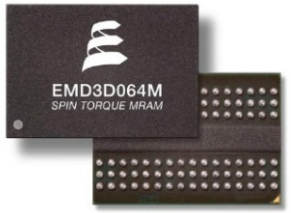

Magnetic censer

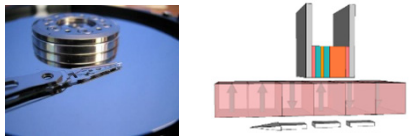

HDD read-out-head

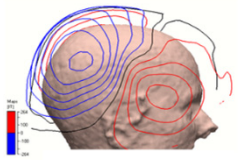

Earth's magnetic field censer・current censer for car・biomagnetic censer

Corresponding to SQUID

Required performance for pMTJs

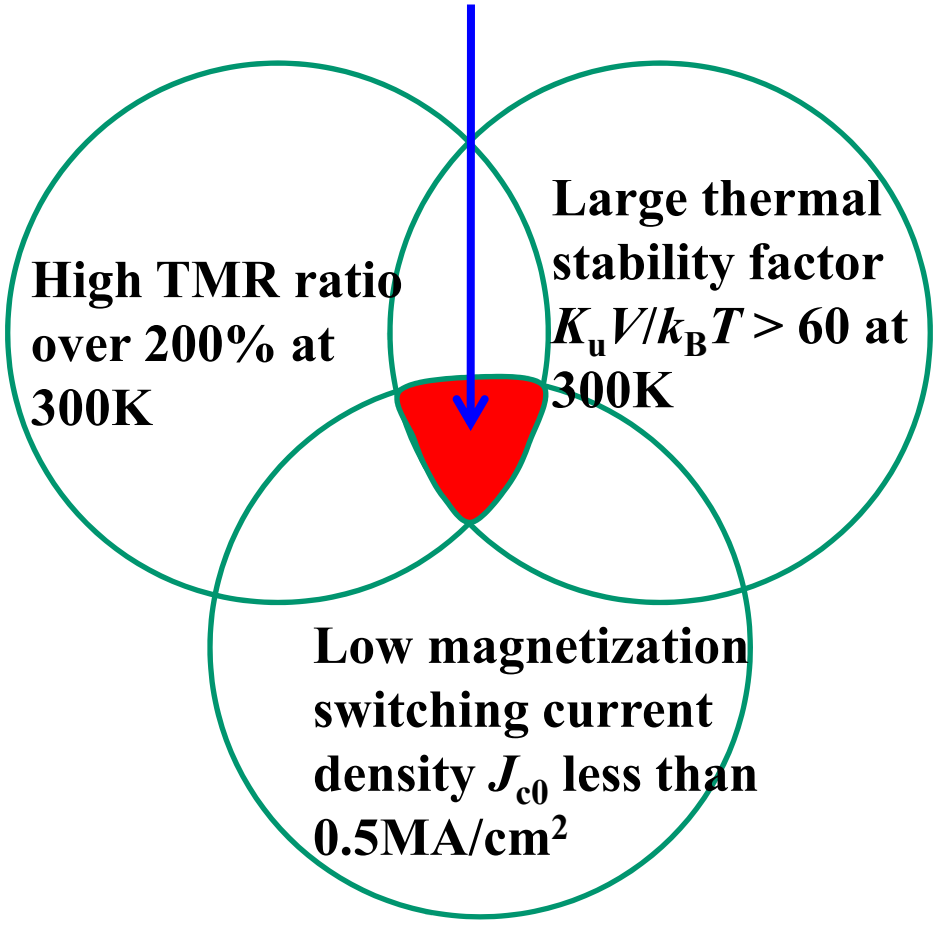

Required properties for spintronic materials